Modelling Advanced Oxidation of Persistent Chlorohalogenated Pollutants in Aqueous Systems

WATER
RESEARCH
COMMISSION

EXECUTIVE SUMMARY

_____

Background

Heterogeneous photocatalytic treatment of organic pollutants in the environment is one of the technologies that has been successful at degrading a wide range of micropollutants. Its success is founded on the ability of semiconductor materials to absorb photon energy at wavelength ranges that allow excitation of surface electrons and subsequent promotion to higher energy orbitals. The exact photocatalytic mechanisms for functional group transformations are not adequately understood in literature, as the reactions associated with heterogeneous photocatalysis are diverse and may include oxidation, cleavage, reduction, geometric and valence isomerisation, substitutions and more.

Aims

The following were the aims of the project:

1. To design and optimise a batch reactor system using systematic preliminary studies on the oxidation of polychlorinated substituted phenols.
2. To perform batch studies and kinetic determinations of the photocatalytic sequence and system performance on the oxidation of polychlorinated substituted phenols in aqueous systems.
3. To determine the reaction mechanism, and, using a sufficient mathematical model, evaluate the performance of the photocatalytic transformations of each chlorophenol

Method

Photocatalytic oxidation reactions are the ones that are better understood when organic substrates are of concern. This study attempted a different approach to photocatalysis of organic compounds, by investigating and evaluating the reductive reaction schemes and their impact towards the degradation of organics in aqueous systems, both in batch and in continuous flow applications. Titanium dioxide (TiO2) was the semiconductor used in the study, while the organic substrates selected for the study were polychlorinated phenolic compounds.

Summary of findings and conclusion

The study conducted experiments on isothermal equilibrium kinetic determinations to calculate each compound's Langmuir kinetics in the photocatalyst adsorption process. The Langmuir-Hinshelwood (L-H) expression was identified as the most plausible to detail the kinetic behaviour of the photocatalytic process. Batch determinations included the investigation the degradation sequence of multi-chlorinated substituted phenols compounds selected, and the kinetic determination and simulations of the simultaneous transformational reductive behaviour of all compounds. Results showed that higher level substituted chlorophenolics degraded at a much faster rate than the less substituted phenolics.

_____

ACKNOWLEDGEMENTS

CONTENTS

_____

_____

LIST OF FIGURES

LIST OF TABLES

_____

_____

This page was deliberately left blank

CHAPTER 1: BACKGROUND

1.1   INTRODUCTION

Improved chemical technology worldwide has been coupled with increased chemical pollutants in the environment. This has been evident in a number of studies conducted in the local environment (Chen et al., 2000). A concerning factor is that the chemical pollutants are not only increasing in diversity but concentration levels in the environment are generally increasing yearly. These emerging pollutants deem current water treatment technologies ineffective at treating or removing the pollutants. This leaves common treated reticulated water undesirable even after treatment. One of the more effective technologies in dealing with emerging pollutants has been the implementation of advanced oxidative processes (AOPs), as they are generally non-selective and completely mineralise most organic chemical species (Angelo et al., 2013; Demeestere et al., 2007; Carp et al., 2004). Though established, this research discipline has not fully reached commercialisation due to technological drawbacks. One advanced oxidative process technology that has shown great potential is photocatalysis. This technology has been proven to completely remove a range of chemical pollutants in mixed reactor aqueous systems. For photocatalysis to reach commercialisation and be readily implemented in water treatment, technological advances to counter the major drawbacks need to be addressed.

Water in many regions of South African and many regions of the African continent is contaminated by organic pollutants or contains harmful pathogens (WHO, 2008). Emerging economies and third world countries cannot afford the majority of high cost environmental remediation technologies proposed in scientific literature, so any remedy needs to be inexpensive, independent of infrastructure power and easy to implement. The direction that is being paved by the advancement of photocatalytic technology and those similar is towards solar power utilisation, but adequate attention needs to be afforded to the fundamental principles and the simplistic manor of its application and relevance to the average economic institution. It needs to also be put into perspective how the proposed alternative measures against conventional water and treatment methods.

AOPs represent an alternative drinking water treatment option to air stripping, granular activated carbon (GAC) adsorption, and resin sorption, methods that are typically used in physiochemical processes (Inagaki et al., 2014; Jin and Dai, 2012; Esparza et al., 2010). Air stripping and sorption are phase transfer processes in which organic contaminants like petroleum additives are physically transferred to a gas phase or solid phase, these are not particularly popular in South Africa. In most physiochemical applications, the actual destruction of long chain organic requires additional processes, such as thermal or catalytic oxidation of the off-gas from an air stripper or incineration of the GAC. In contrast, AOPs destroy primary organic contaminants directly in water through chemical reactions. Several AOP technologies such as ozonation, ozonation combined with H_2O_2, and certain types of UV irradiation are currently used for disinfection purposes in the water treatment industry (Lazar et al., 2012; Lanthasree et al., 2004; Mohseni and Taghipour, 2004), the Daspoort Wastewater

Treatment facility in Pretoria central at some point employed UV as a disinfecting tool in combination with chlorination. Although the use of AOPs for organic contaminant removal from drinking water has been limited in the past, many of the components of AOPs have been used by the water community and industry, however the optimisation of existing systems and installations have only focused on uniquely industrial specialised applications.

1.2   PROJECT RATIONALE

The proposed study puts impetus on the chemical kinetic variability of the transformation potential of related species within the photocatalytic process. Many related and unrelated classes of chemical groups are found dissolved in aqueous matrices, but the typical approach is to identify markers that can represent and be extrapolated into deterministic behaviour (Nugraha and Fatimah, 2013; Oller et al., 2011). This might be plausible in simple applications of the advance oxidation process such as photolysis, where the destruction of the relevant compounds is a function of structural and function group complexity in combination to light source properties. Photocatalysis though a highly promising technology will need to overcome its shortfalls for effective applications, but more importantly its theoretical basis in performance needs to be well understood as very few standard models exist that can be applied from one unique setup to another (Pera-Titus et al., 2004; Pelentridou et al., 2004) . For photocatalysis to realise its true potential the system will need to function in a continuous flow manor, such as the manor current treatment process function in treatment facilities.

1.3   PROJECT AIMS AND OBJECTIVES

The following were the aims of the project:
1. To design and optimise a batch reactor system using systematic preliminary studies on the oxidation of polychlorinated substituted phenols,
2. To perform batch studies and kinetic determinations of the photocatalytic sequence and system performance on the oxidation of polychlorinated substituted phenols in aqueous systems.
3. To determine the reaction mechanism and using a sufficient mathematical model evaluate the performance of the photocatalytic transformations of each chlorophenol

1.4   MODELLING ADVANCED OXIDATION PROCESSES

Modelling semiconductor photocatalytic reaction rates and oxidation mechanisms are based on a number of mathematical statements that can be expressed by sets of ordinary differentials equations, these are sourced and modified from de Lasa et al., 2005. These equations are established for the key chemical species and therefore species' balances in photocatalytic reactors can be typically described as in Eq.1, where V is the total reactor volume.

$$V \frac{dCo}{dt} = \left[\sum_k V_{o,k} \ R_k \ \right] W_{ir}$$

(Eq.1)

Co is the concentration of a singular analyte compound, $V_{o,k}$ is a dimensionless stoichiometric coefficient for the compounds involved in reaction step, k and R_k being the rate of photo-conversion of step k based on the unit weight of irradiated catalyst, Wir. Eq.1 has assumption associated with it, which are;

- o The mass concentration of the catalyst is known.
- o Complete mixing is achieved.
- o The reactor is operated in batch mode.

Eq.1 can be rearranged and simplified, such as in the case of degradation of a single compound. The rate of photooxidation can then be expressed in terms of measurable parameters and variables of that particular pollutant. The consideration of Eq.1 and 2 leads to the advancement of the photocatalytic conversion rate models into a format that is expressed in Eq.3.

$$r_1 = \frac{V}{W_{ir}} \frac{dCo}{dt} = \sum_k V_{o,k} \ R_k$$

(Eq. 2)

$$\frac{dCo}{dt} = \frac{-k_o^m \ C_o}{1 + \sum_{j-1}^{n} C_j K_j}$$

(Eq. 3)

Where ko represents the kinetic constants for the o specie and Kj is the adsorption constant for the species j or any other species present. This reaction kinetic approach takes into account the reactor configuration and the behaviour of the irradiated semiconductor under the system specific conditions. The catalyst surface adsorption concept is viewed as purely dependant on the interaction between the photon and the catalyst mass. This theoretical approach is no different to accepted models that express the heterogeneous photocatalysis mechanism. The most complete of these models is the Langmuir-Hinshelwood expression.

The kinetic modelling is founded on the notion that the degradation processes of individual compounds are coupled with the conversion and formation of derivative species. A higher level substituted chlorophenol is expected to undergo oxidation resulting in the decrease of its concentration, and a subsequent formation of a lower level substituted chlorophenol in combination with other unrelated derivative species. The chemical kinetic variability of the transformation potential of related species required the investigations of chemical compounds with a high degree of relatedness. For empirical purposes, this group of compounds would need to be simple in configuration, be stable, and depict strong reactivity upon initiation under aqueous conditions. Since the effort of this investigation was towards water remediation using photocatalysis, pollutant chemical compounds that have become a significant issue in the chemical treatment sector would not to be identified. One of the groups of compounds of major concern has been the chlorophenols. The transformation of chlorophenols in particular could lead to increase in toxicity of intermediate compounds or end products due to formation of electrophilic metabolites (Michałowicz and Duda, 2007).

Chlorophenols are the group of compounds selected for this study as they generally fit the criteria. A chlorophenol is any organochloride of phenol that contains one or more covalently bonded chlorine atoms. This group comprises of five basic substitution types of phenolics and a total of 19 different chlorophenols. Chlorophenols are prevalent in the environment as they have widespread uses such as being miticides, germicides, algicides, fungicides, and wood preservatives.

The photocatalytic degradation sequence of different chlorohalogenated phenolic compounds will be investigated for the influence of substituted chloride ions on the oxidation efficiency. That which pertains significantly to this study is the theoretical foundations of the photocatalytic behaviour in application to different chemical groups and the lack of unison in scientific literature. The complexity of heterogeneous advanced oxidation is a challenging one in that many steps and reaction mechanism may be operating simultaneously (Yasmina et al., 2014; Pozzo et al., 1997), a simple example to elucidate the complexity of the process is, how kinetic separation of the photolytic process is not possible from that of photocatalysis as these processes happen interdependently (or at least for semiconductor catalyst involvement).

Photocatalysis systems behaviour are mostly speculative, and that is the nature of most intricate science, established models and constructed mathematical models only aid in unravelling more scientific knowledge. This study will attempt to model transformative behaviour of multichlorinated substituted phenols in simultaneous pollutant matrices using kinetic and simulated statistical models. This will provide insight into the dehalogenation sequence and the degradation sequence.

CHAPTER 2: EXPERIMENTAL STUDIES

2.1 INTRODUCTION

This study will attempt to determine the kinetic trail and reaction routes undertaken in the oxidation process towards mineralisation, especially important when dealing with a wide range of organic pollutants that are simultaneously being treated.

2.2 MATERIALS AND METHODS

2.2.1 Chemical standards, reagents and solvents

The phenolics reference standard (P/N: N9331054) inclusive of 4-chlorophenol (4-CP, MCP), 2,4-dichlorophenol (2,4-DCP), 2,4,6-trichlorophenol (2,4,6-TCP), pentachlorophenol (PCP) was purchased from Perkin Elmer (South Africa). Reagents; 4-chlorophenol (99%), 2,4-dichlorophenol (99%), 2,4,6-trichlorophenol (98%), and pentachlorophenol (97%) were purchased from Sigma-Aldrich Logistik GmbH (Schnelldorf, South Africa/Germany). Acetonitrile (99.9%), Dichloromethane (99.9%), Methanol (99.9%), and Acetone (99.9%) solvents were acquired from Merck (South Africa). All solvents used in this study were of either HPLC or GC grade. Anatase titanium dioxide powder (99.8%) and Rutile (99.5%) were purchased from Sigma-Aldrich (South Africa/Germany). Ultra-high purity helium gas (99.99%) was purchased from Afrox, South Africa. All samples were prepared using ultrapure water (UP-water) dispensed by Millipore DirectQ3 (0.05 µS/cm) (Millipore, USA; supplied by MicroSep, South Africa).

2.2.2 Instrumentation and operating conditions

Experimental samples and chemical analysis were conducted using a PerkinElmer Gas Chromatography (GC) system comprising of a Clarus 600 GC, and a Clarus 600 T Mass Spectrometer (MS) (PerkinElmer, South Africa division) (Table 2.1). The GC system injector consists of a split/splitless injector (CHP), a temperature programmed split/splitless injector (PSI), and a temperature programmed on column injector (POC). Sample injections were performed by a multi-mode autosampler comprising of 82 vial multi injection automated rack. The chemical separation component was the Elite 5MS GC and Elite Volatiles system capillary column (30 m, 250 µm) from PerkinElmer and ZB5 Zebron capillary column (30 m, 250 µm) from Phenomenex (Separations Scientific, South Africa). The carrier gas was helium (He) of 99.999% purity. MS interface has an Electron Ioniser (EI), a high performance mass analyser, and a detector consisting of a dynode, phosphor plate and photomultiplier tube. The mass spectroscopy component of the instrument is equipped with time window specifications, these can be coupled with Selected Ion Recordings (SIR). The MS typically scans through a range of masses in very short time spells, with little time spent on each mass fewer ions are collected, this generally limits ion populations and sensitivity.

Table 2.1: GC and MS operating conditions

Component	Type and Settings
GC Oven	
Initial Temperature	40°C
Ramp Rate 1	10°C to 180
Ramp Rate 2	15°C to 240
End	240°C
Autosampler	
Injection Volume	1 µL
Injection Speed	Normal
GC Injector Port	
Temperature	250°C
Carrier Gas	
Flow Rate	1 mL min^{-1}
Split Flow	50 mL min^{-1}
Mass Spectrum	
Mass (m/z)	40-400
Time	GC duration
Ionisation Mode	EI$^+$
Data	Centroid
Scan Time	0.3 s
Inter-Scan Delay	0.02 s
Transfer Line Temperature	250°C
Source Temperature	200°C

When using the SIR process, identified ions are prioritised and a much smaller mass scan range is applied, this significantly improves the detectability of the specified ions. The greater the population of ions, the greater the statistical yield in the spectrum formulation. Mass spectrums are processed against library detailed references, the NIST 2005 library is the software installed. With better resolution of detected chromatograms, certainty is improved and reproducibility in quantification is greatly enhanced.

2.2.3 Ultra-violet irradiation sources

Ultra-violet irradiation sources were the long-arc 400 W lamps (Philips HOK 4/120 SE), medium pressure 36 W lamps (Philips TUV 36), and the 75 W lamps (Philips TUV 75) (Philips Netherlands). Goldilux UV Smart Meters (Model GRP-1) equipped with UV-A, UV-B and UV-C probes (Table 2.2) and were purchased from Measuring Instruments Technology (MIT) (South Africa). The pH and temperature were measured using a Hach HQ11d meter (Aqualytic Environmental & Laboratory, South Africa). Gas flow meters (0-100 mL min^{-1}). Oxygen (99.99%), nitrogen (99.99%) and argon (99.99%) were supplied by Afrox (South Africa).

Table 2.2: Measured UV Lamp properties

Lamp	Wattage (W)	UVA (μW/cm^2)	UVB (μW/cm^2)	UVC (μW/cm^2)	Voltage (V)
HOK 4/120	400	687.45± 19.05	20.70 ± 0.646	51.37± 2.021	125
TUV 75	75	28.05± 0.128	45.48± 0.568	3672± 5.86	103
TUV 36	36	20.30± 0.415	26.45± 0.08	2419± 8.05	110

2.2.4 External standards calibrations

Chemical reference standards were used to develop the GC-MS methods and to perform analytical method processing. The five analytes retention times were determined and chromatograms outputs were re-processed for resolution optimisation. Chemical reagents were used to prepare the relevant stock solutions in the appropriate solvent mixtures. Linear concentration ranges were confirmed to be within the working experimental ranges. The different analyte peak chromatogram responses differed between the low mass and high mass analytes, therefore slightly different concentrations were calculated and prepared for calibrations response optimisation. All compound mass concentrations ranged between 0 and 20 mg L^{-1}, even with periodic changes in GC-MS capillary columns between the Elite semi-volatile and the Elite volatile types.

2.3 BATCH EXPERIMENTAL STUDIES

2.3.1 Reactor setup

The photocatalytic process was conducted in the setup presented in Figure 2.3. The reactor vessel had a 1 L capacity up to the solution level indicated in Figure 2.1, it rested on a magnetic stirrer with an rpm setting of 200. 15 cm on either side of the vessel were quarts sleeved long-arc UV lamps (Phillips HOK 4/120 SE, 400 Watts). A fizzling oxygen tube attached to a flow regular, sensor probe (HQd MTC 101), and a glass sampling tube attached to precision pump tubing (Masterflex) on the top end were immersed into the vessel. The setup was installed in a temperature regulated walk-in reactor room that is wall-connected to a cold-room of 4°C set temperature, the wall connection has small port-openings that allow transfer of cooled air. Installed inside the reactor room in a fan-driven vacuum cooling system.
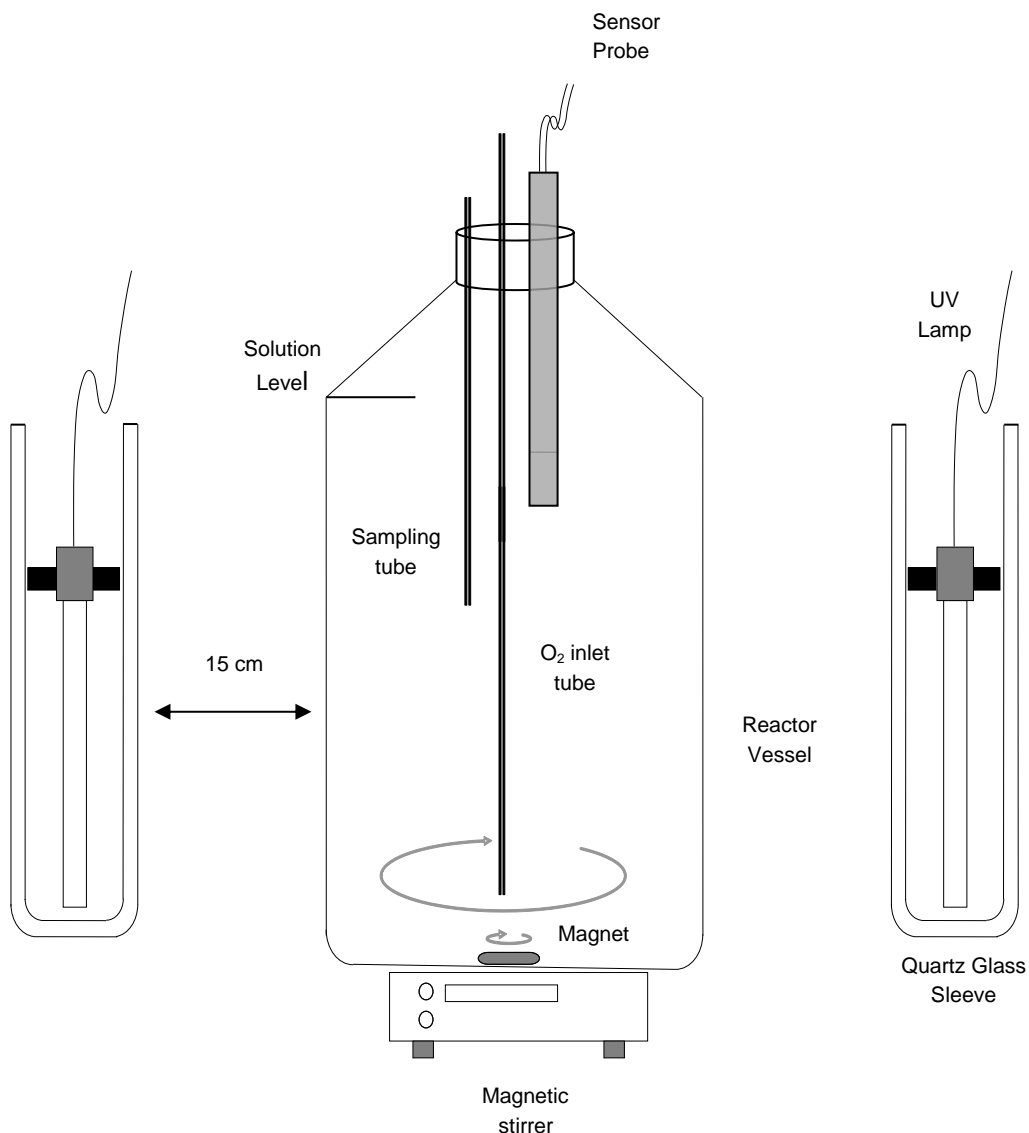
Figure 2.1: Schematic of the laboratory photocatalytic reactor setup

2.3.2 Experimental process

The reactor setup process included solution temperature determinations over the irradiation period, this was conducted by control pseudo-experimental runs using water solution. It was determined that at shorter distances the irradiation intensity was enough to offset the reactor room cooling system. There was a relationship between the fractional increases in solution temperature and the distance of the radiation sources. Progressive increases in UV lamp distances were conducted to determine the distance at which the solution temperature would remain relatively unchanged. The distance of 15 cm from the outer surface of the vessel and the outer surface of the quarts sleeve was determined to be the minimum distance required not to interfere with cooling, this is depiction in Figure 2.1. Analyte spiked solution were prepared accordingly, catalyst dispensation took place after chemical application, this was followed by sonication (8891 Cole-Parmer) for 10-15 minutes. Oxygen flow (20 mL min^{-1}) was initiated prior to solution transfer, only when the system was

set did the UV irradiation take place. 1.5 mL sample volumes were removed at predetermined intervals, centrifuged (eppendorf minispin) for 20 minutes at 5000 rpm before instrumental analysis.

2.3.3 Determination of titanium dioxide semiconductor morphology

Anatase titanium dioxide was analysed using a high resolution scanning electron microscope (SEM) (Joel, JSM-5800LV). The oxide particles were prepared for viewing by coating on carbon plates using the standard method. The purpose of this exercise was to determine whether there was morphological change of the particle structure before application to the photocatalytic treatment of analytes and after several applications, and to visually determine and measure the size of particles using micrograph scale to determine oxide particle aggregation after several applications.

2.3.4 Kinetic adsorption equilibrium isotherm

Adsorption isotherms were determined by accurately weighed anatase titanium dioxide (30 mg L^{-1}) dispensed in aqueous chlorophenols spiked (5, 10, 15 20, 25 mg L^{-1}) solutions (0.5 L) continuously stirred at 300 rpm. Pentachlorophenol has a low solubility in aqueous solutions (20 mg L^{-1} at 30°C), therefore lower chemical concentrations within the PCP solubility range were used, as given above. The temperature was controlled at 19°C. The resulting pH of the solutions was in within the range of 5.4 to 5.7. The solutions were agitated for over 20 hours to reach equilibrium. After a minimum period of 20 hours samples were removed and centrifuged (eppendorf AG minispin) for 30 minutes at 5000 rpm. Sample residual concentrations were analysed using the GCMS. Experiments were repeated and average values are reported. The Langmuir isotherm model was used to determine and calculate adsorption parameters. The Langmuir isotherm equation is given as:

$$Q_e = \frac{Q_m K_L C_e}{1 + K_l C_e}$$

(Eq. 4)

where Q_e is the adsorbed chemical concentration per weight of adsorbent at equilibrium (mg g^{-1}), C_e is the final equilibrium solution concentration (mg L^{-1}), K_L is the free energy Langmuir adsorption constant (mg L^{-1}), and Q_m is the maximum adsorption capacity (mg g^{-1}). Eq.*4* is linearised to Eq.*5*.

$$\frac{1}{Q_e} = \frac{1}{Q_m K_L C_e} + \frac{1}{Q_m}$$

(Eq. 5)

The plots of the inverse of the adsorbed chemical concentration per weight (Q_e) versus the inverse of the final equilibrium solution concentration (C_e) are used in the study and processing of the kinetic calculations.

2.3.5 **Modelling and statistical software**

Sigmaplot 11 (Systat Software, San Jose, CA) scientific data analysis graphics computation software was used for data processing and statistical analysis. The program was designed for the identification and simulation of aquatic systems in the laboratory, in technical plants, and in nature. The program is used to simulated experimental data profiles using derived and known expressions through mathematical modelling. Kinetic parameter estimations are conducted with input values and constraints determinations. Calculated error estimations are used to perform model sensitivity analysis.

2.4 RESULTS AND DISCUSSION

2.4.1 **Titanium semiconductor morphology**

Figure 2.2 and Figure 2.3 suggest that there are no obvious morphological structure differences before application and after usage. From the measurement of several (n=10) random particles on both images there was no conclusive difference in size, but a higher degree of aggregation is observed in Figure 2.2.
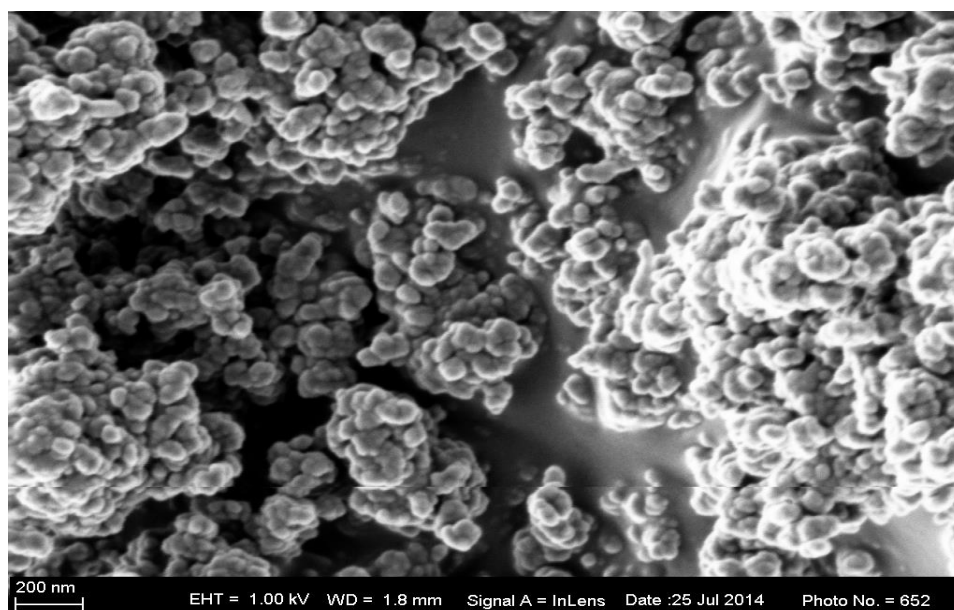
Figure 2.2: SEM image of anatase titanium dioxide particle before application
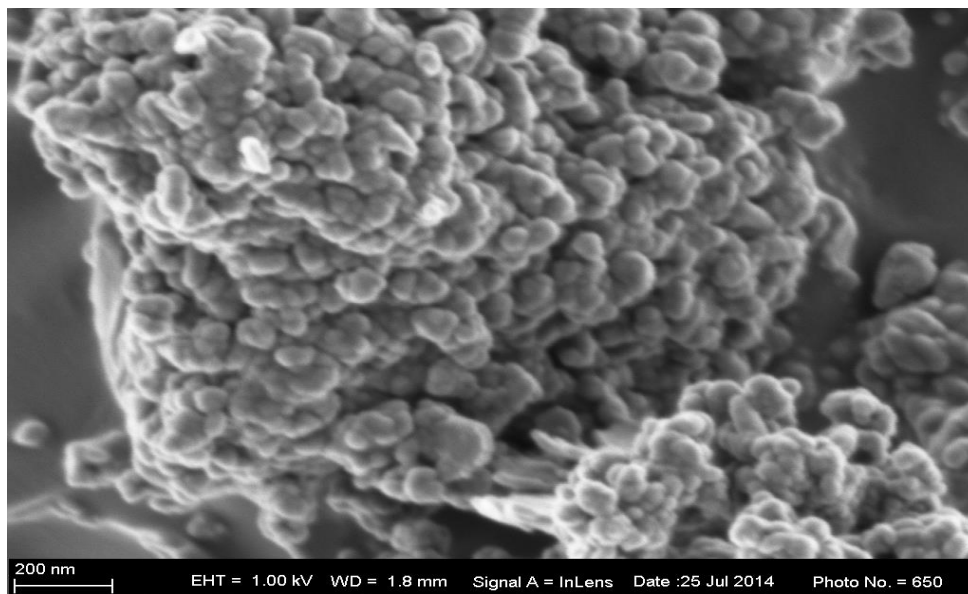
Figure 2.3: SEM image of anatase titanium dioxide particle after application

2.4.2 Kinetic adsorption equilibrium isotherms

The experimental kinetic adsorption isotherms of the chlorophenols and phenol onto the titanium dioxide photocatalyst are presented in Figure 2.4. Table 2.3 presents the calculated parameters for the adsorption of the phenolic compounds onto titanium dioxide surface sites. With the exception of phenol, the four chlorophenols appear to be adsorbed onto the photocatalyst in concentrations directly proportional to their degree of chlorination. A study by Hamdaoui and Naffrechoux (2007) reported similar findings on surface adsorption isotherms of similar compounds. Zhonghua and Vansant (1993) suggested that the adsorption of phenols in aqueous solutions can be related to their hydrophobicity's when examining phenol, monochlorophenol, dichlorophenol and trichlorophenol.
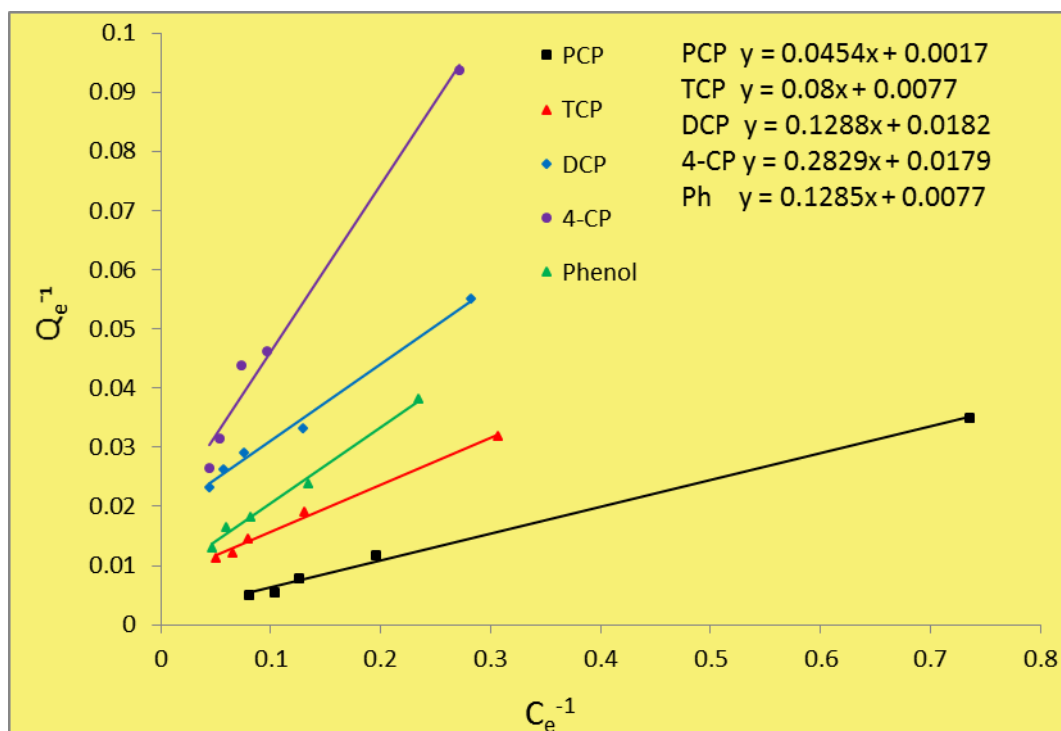
Figure 2.1: Langmuir isotherm plots for pentachlorophenol, trichlorophenol, dichlorophenol, chlorophenol and phenol.

Table 2.3: Parameters of the Langmuir isotherms for the adsorption of phenolic compounds onto TiO$_2$

Isotherm	Phenol	MCP	DCP	TCP	PCP
K_L (mg L^{-1})	0.0603	0.0676	0.1420	0.0987	0.0390
Q_m (mg g^{-1})	130.01	57.470	55.860	130.02	588.20
R^2	0.9919	0.9839	0.9913	0.9938	0.9956
Stdev	0.0060	0.0149	0.0155	0.00984	0.00595

The study stated that the adsorption capacities and affinities can be related to the number of chlorine atoms substituted to the phenol structure, and reported an adsorption sequence of; phenol < chlorophenol < dichlorophenol < trichlorophenol. According to Giles et al., 1960, the nature of curvature shape observed in the experiments indicates that as more sites in the substrate are filled it becomes increasingly difficult for a bombarding solute molecule to find vacant sites. Though the range of adsorption profiles in the current study is smaller than that investigated by Hamdaoui and Naffrechoux (2007), the findings show a similar pattern for monochlorophenol, dichlorophenol and trichlorophenol. Excluding phenol, the order of adsorption onto titanium dioxide in the current study was; monochlorophenol < dichlorophenol < trichlorophenol < pentachlorophenol. The plots of the inverse of the adsorbed chemical concentration per weight (Q_e) versus the inverse of the final equilibrium solution concentration (C_e) were used for studying the adsorption data. The Langmuir adsorption constants (K_L) for all compounds were calculated as recorded in Table 2.3.

2.4.3 **Preliminary experimental findings**

2.4.3.1 *The impact of the photocatalyst*

The first point of interest with regards to preliminary studies was to determine whether the inclusion of the semiconductor photocatalyst does in fact improve the oxidation reactions towards complete mineralisation. For this part of the study 2,4-dichlorophenol was used as the tracking chlorophenol compound, reason being that it has the highest dissolution in aqueous solutions of the compounds selected.

All parameters were kept constant while progressive increases of the photocatalyst were applied with each experiment, to a point where the highest efficiency was measured. Figure 2.5 shows DCP oxidation profiles at different catalyst loads. The photolytic process achieved the least efficiency of removal and registered 55 percent reduction in DCP concentration after an irradiation period of a complete 80 minutes, while the best performing experimental set recorded complete reduction of DCP in less than 40 minutes of irradiation.

Figure 2.5 shows that the inclusion of the photocatalyst gradually improves the rate of DCP oxidation until a certain critical concentration, beyond which the system performance is impaired. In the current investigations the critical catalyst loading is between 26 and 34 mg per litre catalyst. The efficiency of reduction is compromised beyond 30 mg L^{-1}. A systematic and gradual decline in efficiency is recorded, and expected to maintain the trend until photon delivery is completely compromised.
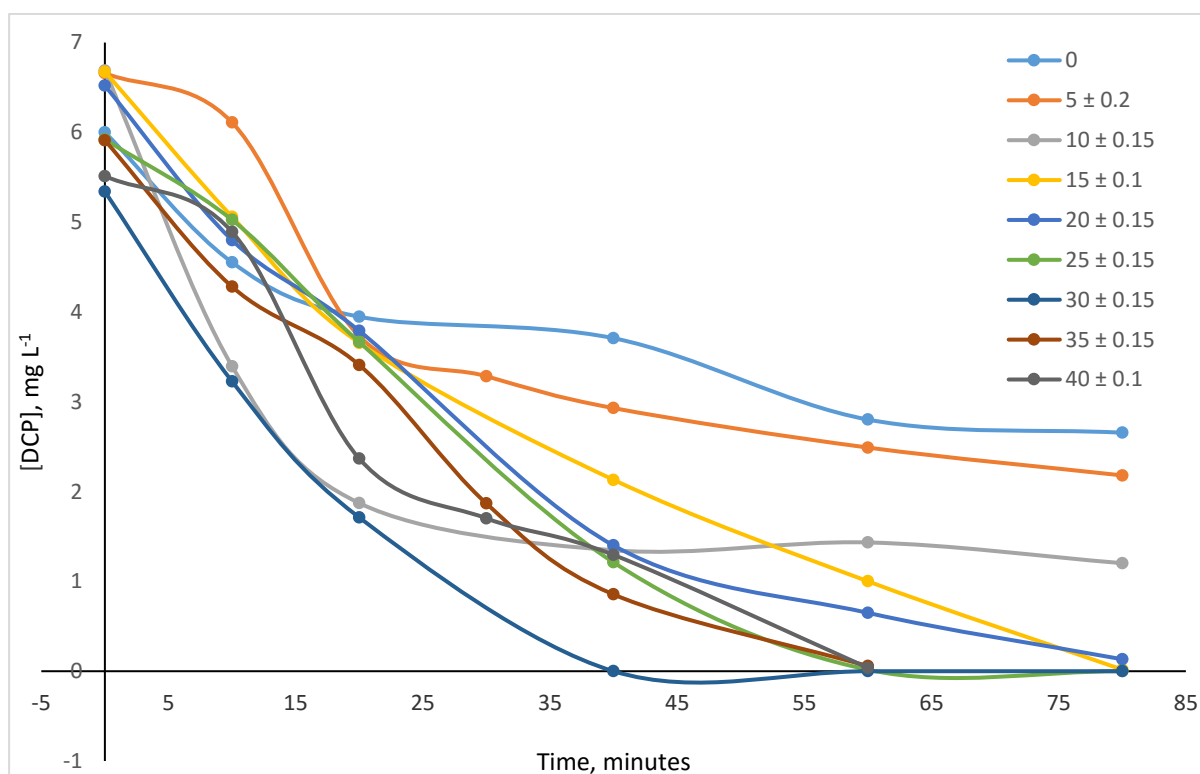

Figure 2.2: The photodegradation of DCP versus changes in catalyst concentration [pH 5, Oxygen flow-rate 20 mL min^{-1}].

2.4.3.2 The influence of pH

It was empirically determined that the 30 mg L^{-1} catalyst loading was the most efficient for the photocatalytic degradation of DCP under conditions up to that point at pH 5. It was thus important to determine the influence of pH levels versus the photodegradation of the DCP. Sulphuric acid and sodium hydroxide were used to set the desired pH levels of the solutions.

Figure 2.6 shows the DCP oxidation profiles when pH values are manipulated. Results suggest that solution matrix pH levels have a marked influence on the photocatalytic rate of reactions. Findings indicate that the rate of degradation reactions is decreased with decreases in pH setting below pH 5. It is interesting to note that pH 4 experimental sets recorded the least efficient pH range, this suggests that different ranges of pH levels may uniquely effect the rate of oxidation.

The pH 6 degradation profiles recorded less efficiency of DCP removal in comparison to pH 5 and others, for this reason it was deemed that pH 5 is the optimum range required to effective oxidise chlorophenols in aqueous solutions. All official experimental data were acquired using solution preparation in the pH 5 range.
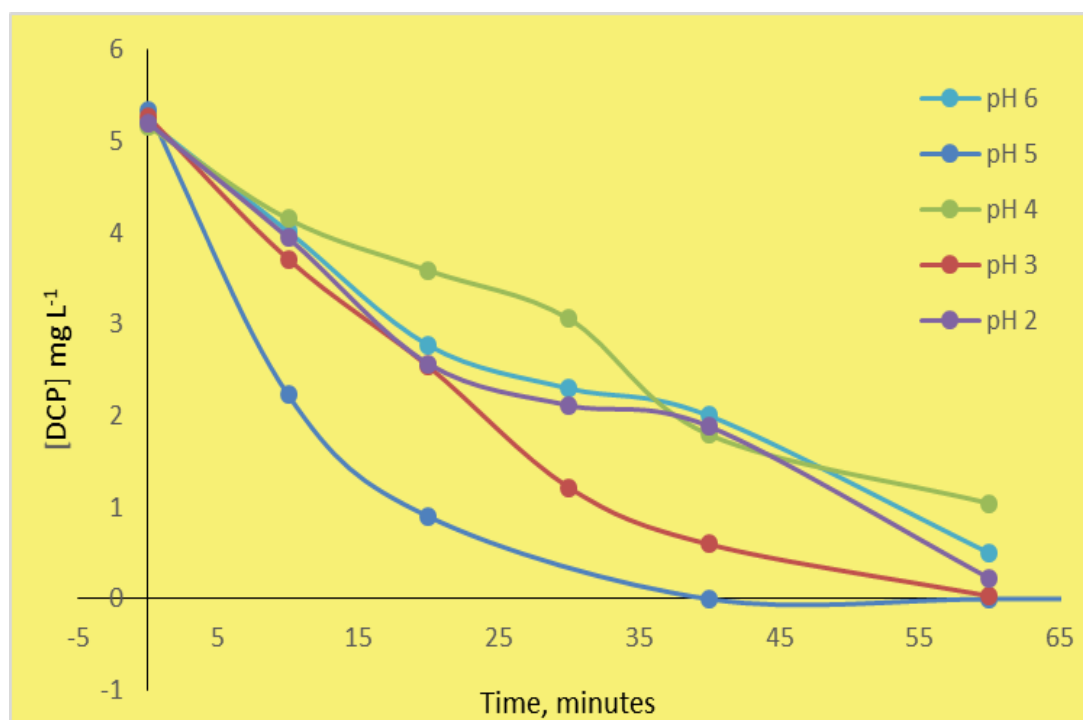

Figure 2.3: The photodegradation of DCP versus pH changes. [TiO$_2$] 30 mg L^{-1}, Oxygen flow-rate 20 mL min^{-1}].

2.4.3.3   The effect of oxygenation

Photoexcitation of semiconductor photocatalysts in the ultra-violet region of the light spectrum generates electron hole pairs that rapidly recombine with subsequent release in absorbed energy. In the presence of trapping charges in the form positive or negative ion moieties, the generated electron are snatched or scavenged by the electron donor and electron acceptors, these results in prevention of recombination. The electron-hole pair generation and recombination process takes place in a few tens of picoseconds.

Pure oxygen or compressed air are typically used to trap the generated electrons. The TiO_2 conduction band edge reduces oxygen to generate highly oxidative radicals $O_2^{\circ-}$. This is one of the reasons titanium dioxide is the most efficient semiconductor catalyst, and the limitations of other semiconductors.

Two sets of controls were included in the determinations. In the one set, the system was not oxygenated and only the oxygen that was naturally dissolved in solution remained. The other control included active removal of oxygen molecules from the system through continual purging using a noble gas (Ar), this is meant to devoid the system of all forms of oxygen including molecules that are by-products of the oxidation process. Figure 2.7 shows the performances of each of the manipulations of the electron acceptor and the effects with regards to photocatalytic oxidation of DCP. Recorded is the progressive improvements of the photocatalytic process with increases in available oxygen molecules.
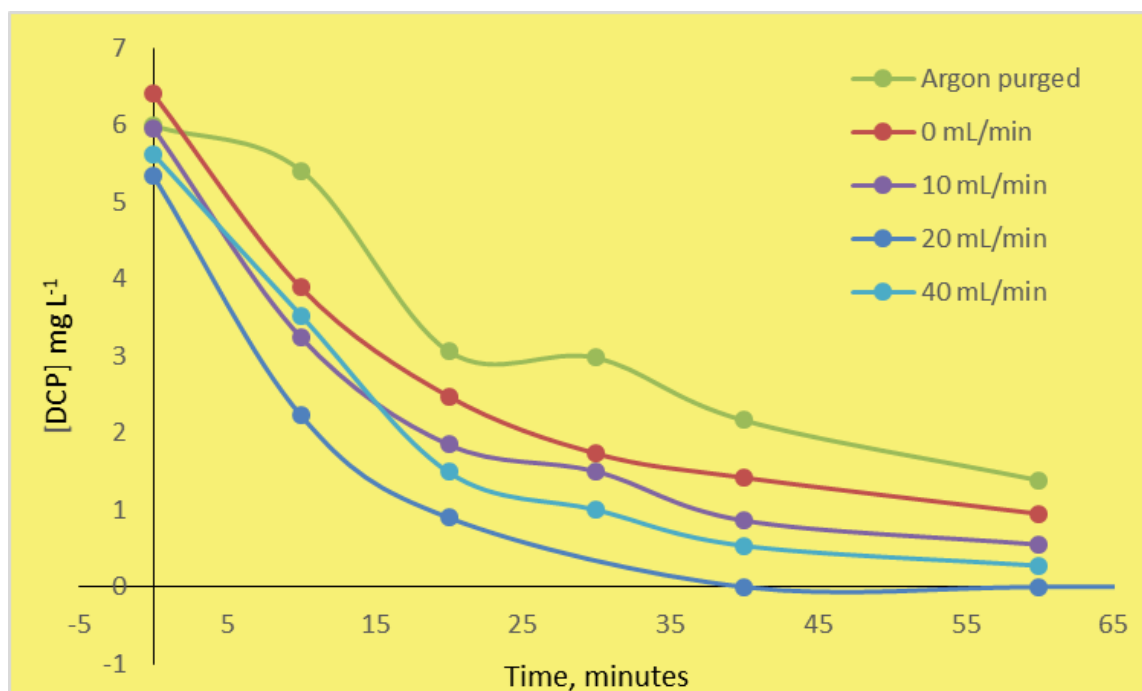

Figure 2.4: The photocatalytic degradation of DCP versus oxygenation and purged sets. [TiO$_2$] 30 mg L^{-1}, pH 5].

It was found that the photocatalytic rate of degradation improved with increased amount of available oxygen to the system. It was also observed that at 40 mL min^{-1} and higher the vigorous nature of gas bubbling affected

the integrity of the matrix solution through turbulence and destruction mixing. The 20 mL min^{-1} setting was thus preferred and used in the rest of the investigations.

A basic batch study was undertaken using dichlorophenol as the chlorophenol of interest. This part of the preliminary determination also included an informative control. The control determination was once again continuous argon purging. Continuous pure nitrogen (N_2) gas bubbling into the spiked matrix solution was applied as a potential electron acceptor, this was meant to depict the effective nature of oxygen as an electron scavenger. The efficiency of pure dissolved oxygen (99.999 %) was the parameter under investigations in the validation of electron scavenging in the photocatalytic performance of DCP degradation. When argon was continuously introduced to the solutions to devoid the system of any dissolved and generated oxygen molecules, this would essentially promote electron-hole pair recombination and reduce the efficiency of the photocatalytic process. Figure 2.8 confirms expectation that the Ar purged profile managed a dichlorophenol reduction of 39 percent in 80 minutes of irradiation. The reduction in DCP concentration can be assumed to be minimally contributed to by photocatalysis, direct photolysis may be attributed to the chlorophenol oxidation.

To elucidate oxygen as a viable electron acceptor, nitrogen diatomic gas was continuously introduced to the solution. Nitrogen in its molecule state (N_2) is not readily reactive and naturally has to go through microbial mass facilitation and through a series of intermediate gaseous nitrogen oxide products before achieving viable oxidising properties. The results in Figure 2.8 suggest that the recombination process is somewhat suppressed by the inclusion of nitrogen but not to the extent of argon purging, 68 percent dichlorophenol was oxidised in 80 minutes of irradiation. Over 98 percent of DCP was reduced in 40 minutes of UV exposure under oxygenation, proving the effectiveness and importance of an electron scavenger to heterogeneous semiconductor photocatalysis.
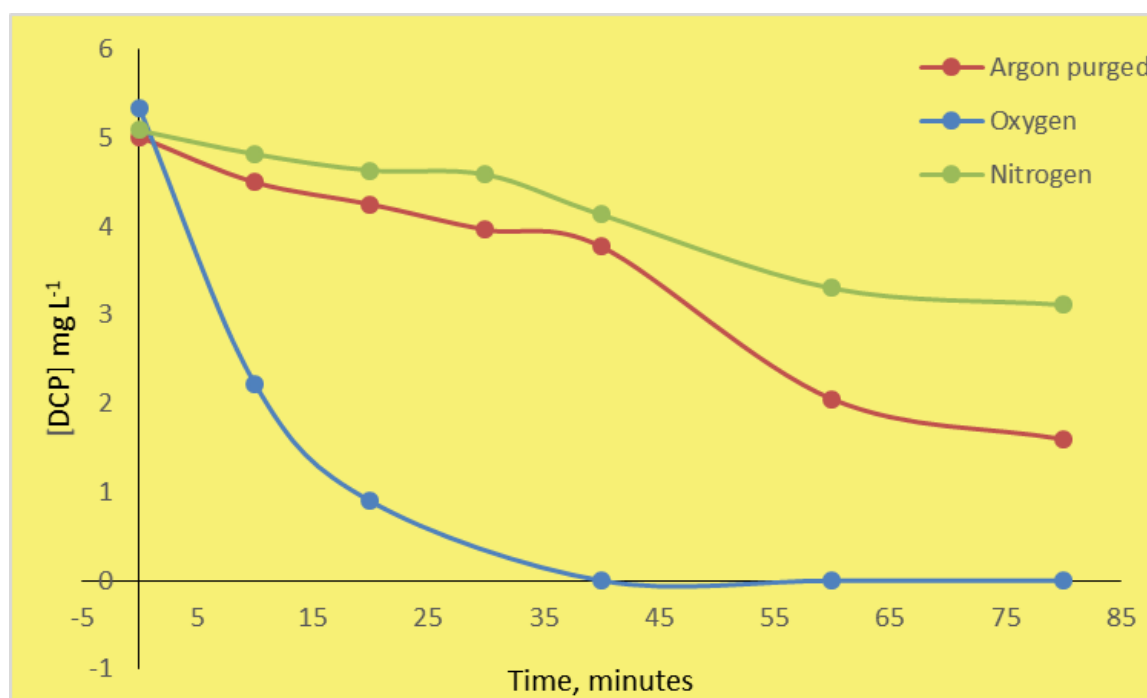
Figure 2.5: The photocatalytic degradation of DCP versus electron acceptors. [TiO$_2$] 30 mg L^{-1}, pH 5. Flow rate 20 mL min^{-1}.

2.4.4 Titanium dioxide isomers

Titanium dioxide occurs naturally in the form of three different polymorphs, namely, anatase, rutile and brookite. The most common are anatase and rutile, they have a tetragonal lattice and are more stable at ambient conditions, while brookite has an orthorhombic structure and significantly less stable. The band gap of TiO$_2$ is larger than 3 eV (~3.0 for rutile and ~3.2 for anatase), thus making pure TiO$_2$ primarily active for UV light.

Anatase is generally accepted to be more active than rutile and is regarded as superior for various properties including that it has a larger band gap than rutile TiO$_2$. While this reduces the light that can be absorbed, it may raise the valence band maximum to higher energy levels relative to redox potentials of adsorbed molecules. This increases the oxidation 'power' of electrons and facilitates electron transfer from the TiO$_2$ to adsorbed molecules (Batzill, 2011).

The nature of the study dictated that it be important to confirm and verity the performance of the two predominantly used titanium dioxide polymorphs in the preliminary studies. Figure 2.9 shows the performance efficiency profiles of anatase and rutile forms of the photocatalyst. It is evident from Figure 2.9 that the anatase polymorph is a much better semiconductor than the rutile, where a total of just over 80 percent of DCP was reduced after irradiation of 80 minutes, whilst compete disappearance of DCP was in achieved in half the period in the anatase experimental sets.
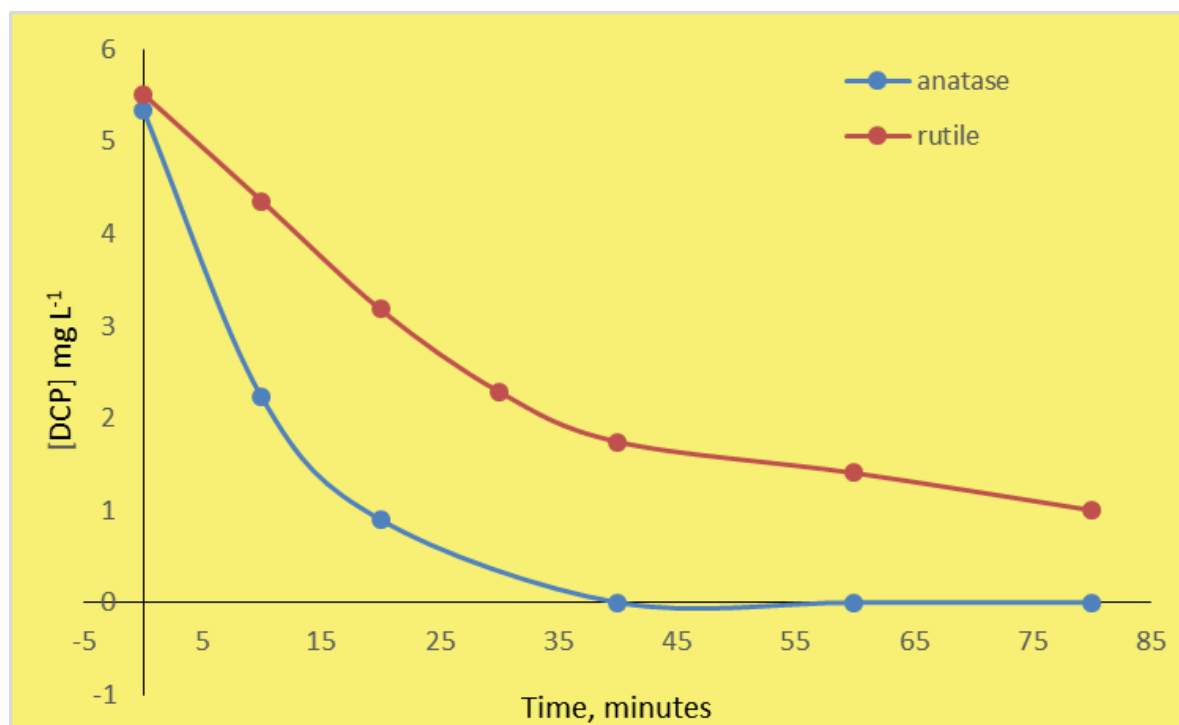
Figure 2.6: The photocatalytic degradation profiles of DCP using anatase and rutile isomers of the photocatalyst. [TiO$_2$] 30 mg L^{-1}, pH 5. Flow rate 20 mL min^{-1}.

2.4.5 The impact of UV light intensities

Table 2.4 shows the properties of the UV lamps used to deliver the adequate range of UV light for the photodegradation of DCP under all mentioned experimental conditions. The HOK 4/120 lamps photon delivery achieved the most efficient photocatalytic removal of the compound of interest, performing significantly better than the lesser Wattage lamps. The TUV lamps were relatively of consistent design barring the delivered Wattage and variations in the UVA, UVB, and UVC ranges. There was little difference in the TUV lamps (75 and 36 W) at the beginning stages of the photodegradation process (Figure 2.10). It is however obvious that at longer treatment periods that there emanates performance discrepancies between the two, where the higher wattage delivery lamp maintains performance while the lower wattage lamp experiences impaired performance.

Table 2.4: Ultra-violet radiance properties

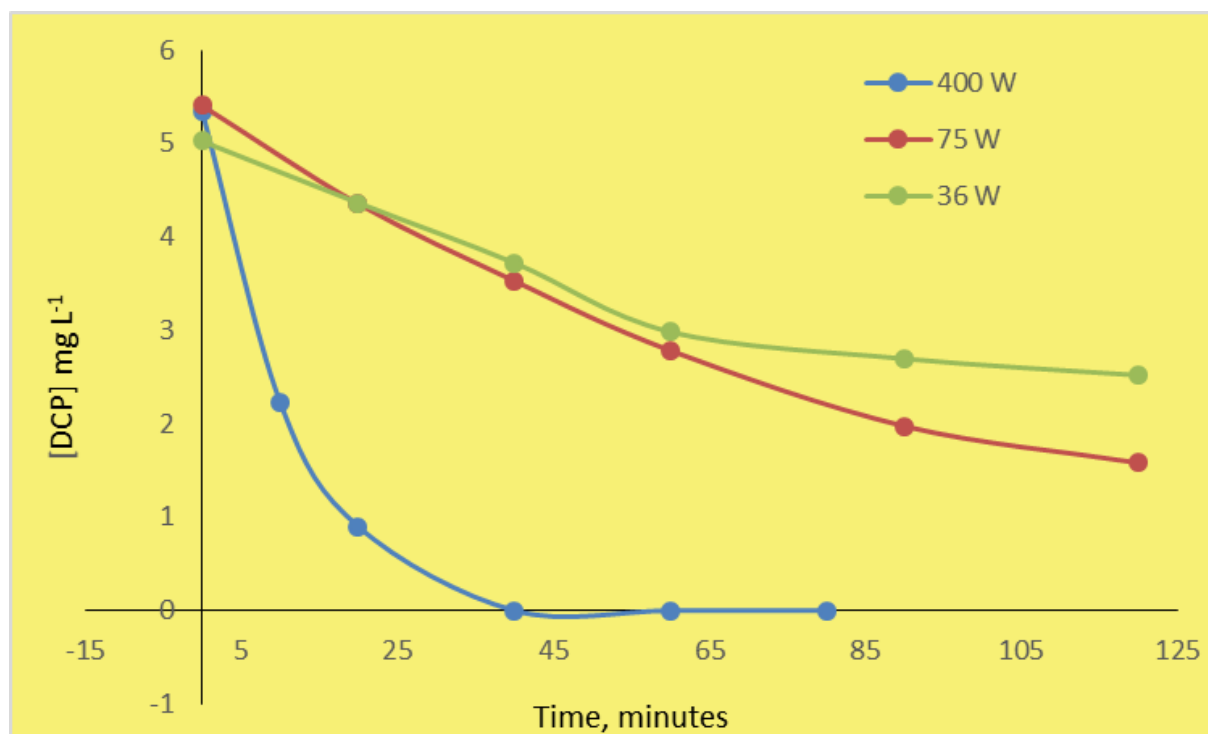| Lamp	Wattage (W)	UVA (μW/cm^2)	UVB (μW/cm^2)	UVC (μW/cm^2)	Voltage (V)
HOK 4/120	400	687.45± 19.05	20.70 ± 0.646	51.37± 2.021	125
TUV 75	75	28.05± 0.128	45.48± 0.568	3672± 5.86	103
TUV 36	36	20.30± 0.415	26.45± 0.08	2419± 8.05	110

Figure 2.7: The photocatalytic degradation profiles of DCP at different light intensities. [TiO$_2$] 30 mg L^{-1}, pH 5. Flow rate 20 mL min^{-1}].

2.4.6 Singular chlorophenols oxidation time course

All the chlorophenol compounds treated individually behaved in a manner that suggested relation to the number of substituted chloride halogens, this is evident on the concentration versus time based profiles. Increases in complexity of the molecular structures are paralleled with decreases in oxidation efficiency. Figures 2.11-2.15 show the graphical representations of the four chlorophenols and phenol's photocatalytic behaviour in aqueous matrices. Kinetic reaction orders were determined using the Langmuir-Hinshelwood heterogeneous reaction model.

The L-H equation can be simplified to a pseudo-first order equation at low organic chemical concentrations. The plot of the logarithm of the concentration ratio (C$_0$/C) versus reaction time yielded a straight line, the slope of which upon linear regression equals the apparent first-order rate constant. In-depth detail of the Langmuir-Hinshelwood expression is extensively discussed in proceeding subsections. First-order rate of reactions were recorded for all the compounds under study. The kinetic rate constants calculated from the data plots correlate to the oxidation profile time course, where excluding phenol, the values descend with increased chlorohalogenated substitution.

Figure 2.8: Fitted kinetic rate constants of PCP photocatalytic oxidation

Figure 2.9: Fitted kinetic rate constants of TCP photocatalytic oxidation

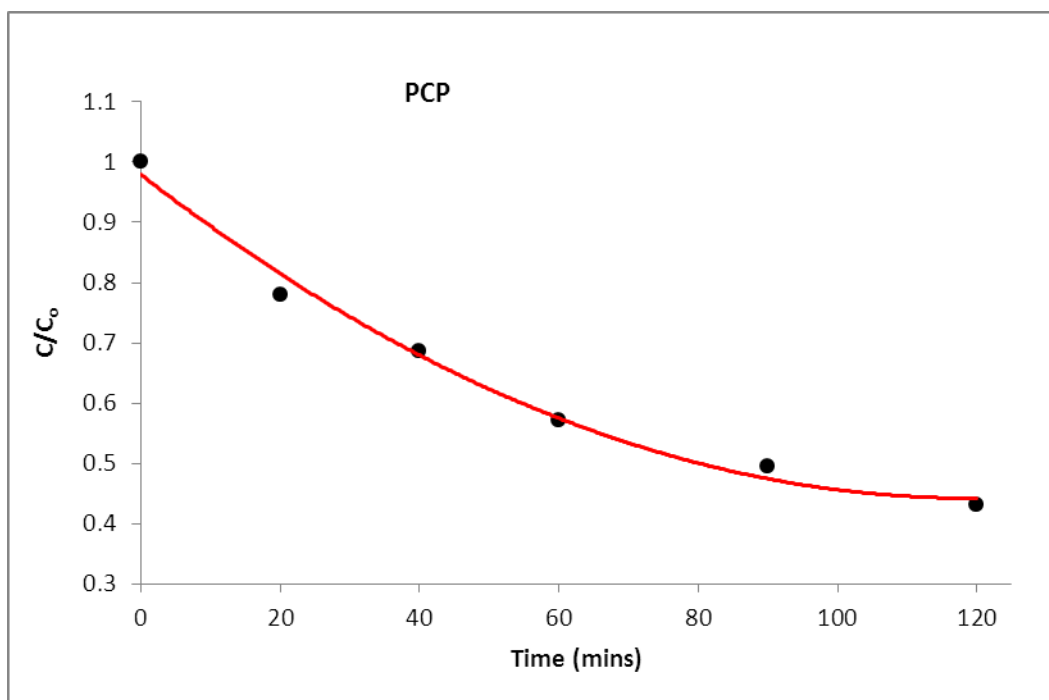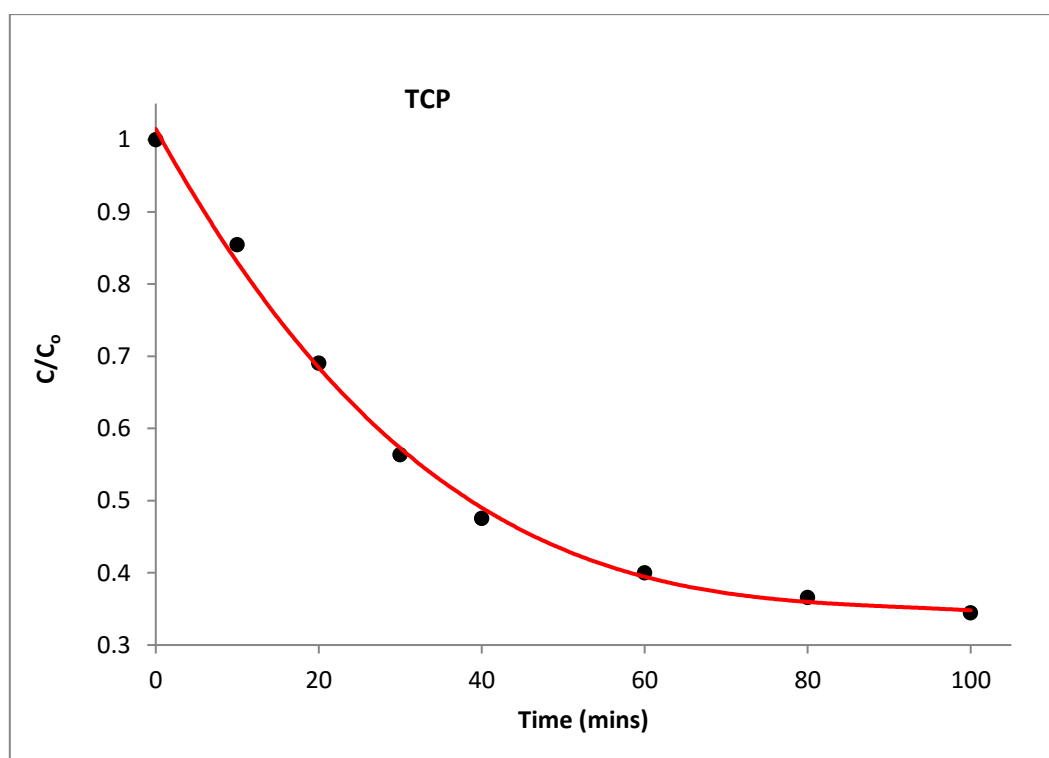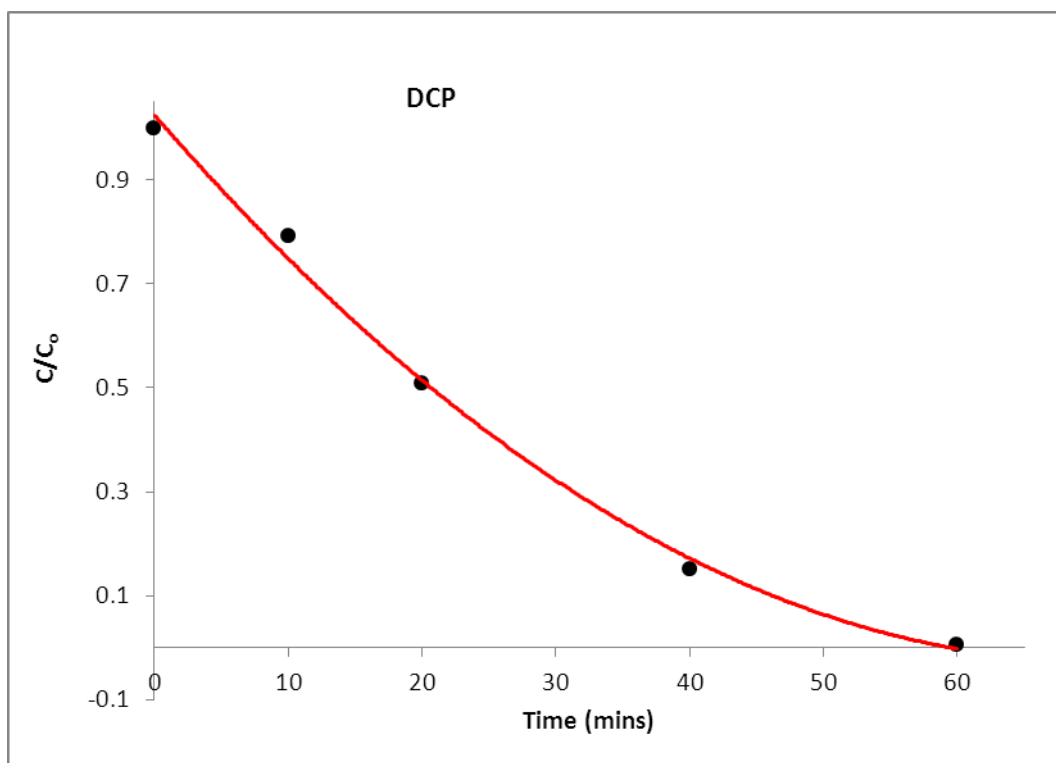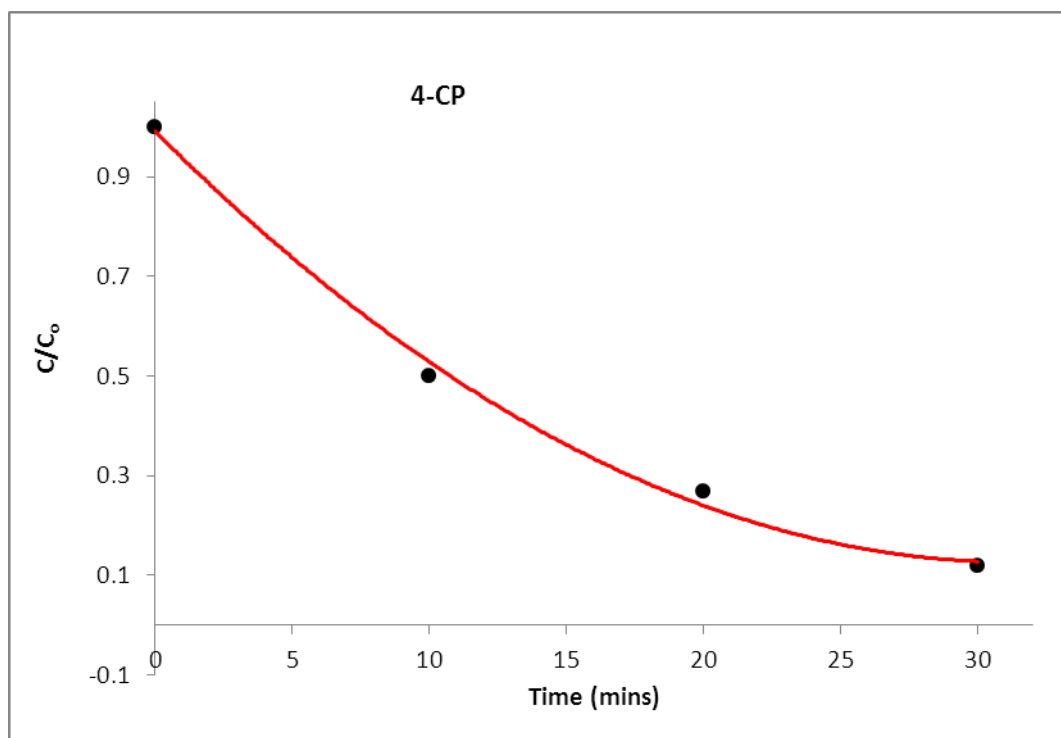**Figure 2.10:** Fitted kinetic rate constants of DCP photocatalytic oxidation

Figure 2.11: Fitted kinetic rate constants of MCP photocatalytic oxidation
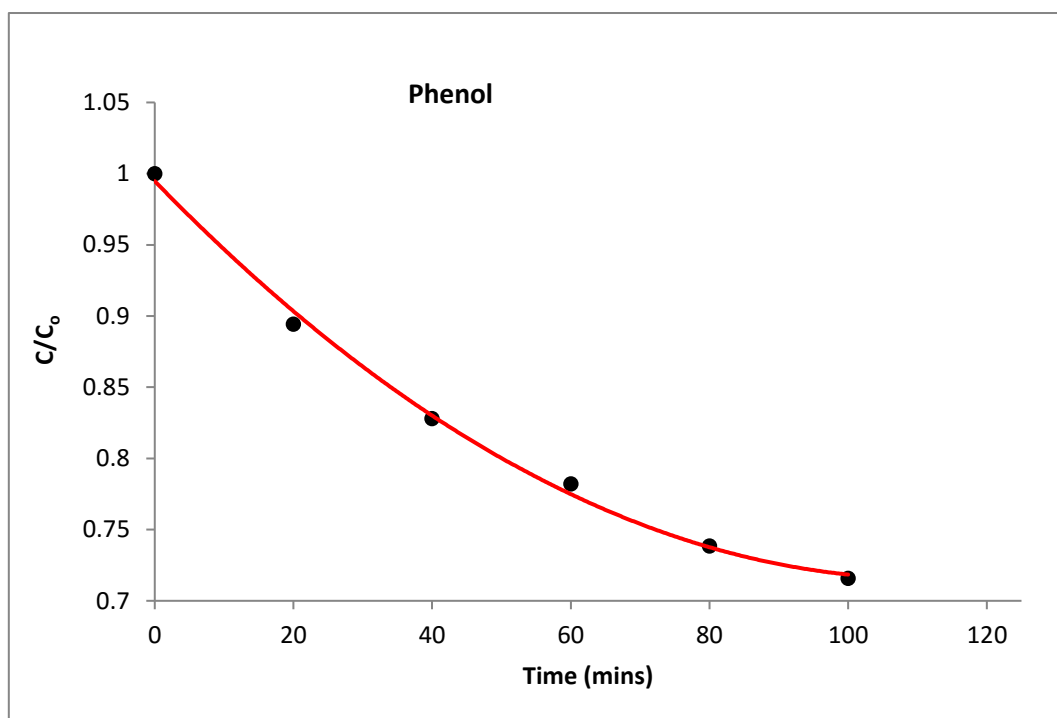
Figure 2.12: Fitted kinetic rate constants of phenol photocatalytic oxidation

2.4.7 Simultaneous chlorophenols dehalogenation oxidation sequence

Few investigations have been conducted on the behaviour of chloride-halogen substituted phenol compounds simultaneously degraded photocatalytically. Studies on the advanced oxidation process of simultaneously degraded chlorinated phenolic compounds present an unclear picture of the degradation sequence of the compounds. Song-hu and Xiao-hua (2005) obtained a Fenton's reagent sequence of 2,4-DCP > 2,4,6-TCP > PCP > 4-CP, Bandara et al., 2001 obtained a 2,4-DCP > 2-CP > 2,3-DCP > 2,4,6-TCP photocatalytic degradation sequence, and Benitez et al. (2000) recorded a sequence of 2,3,4,6-TeCP > 2,4,6-TCP > 2,4-DCP > 4-CP under ozonation. Data from preliminary experiments of this study suggested the contrary, that the oxidation sequence in the photocatalytic process may be reversed. The hypothesised mechanism is that the degradation processes of individual compounds are coupled with the conversion and formation of derivative species. A higher level substituted chlorophenol is expected to undergo oxidation resulting in the decrease of its concentration, and a subsequent formation of a lower level substituted chlorophenol in combination with other unrelated derivative species. This is in contrast to findings in studies where the photocatalytic process resulted in higher chloride halogenated phenols recording slower rates of degradation and contrary to expectation where simpler organic compound complexes are typically broken down faster and easier than higher organic group complexes. Experimental batch reactor investigations were conducted to determine the photocatalytic dehalogenation sequence of the four chloride substituted phenolics and phenol in aqueous systems. Figure 2.16 shows the acquired oxidation profiles of all analytes with initial chemical concentrations of 5 mg L^{-1}.
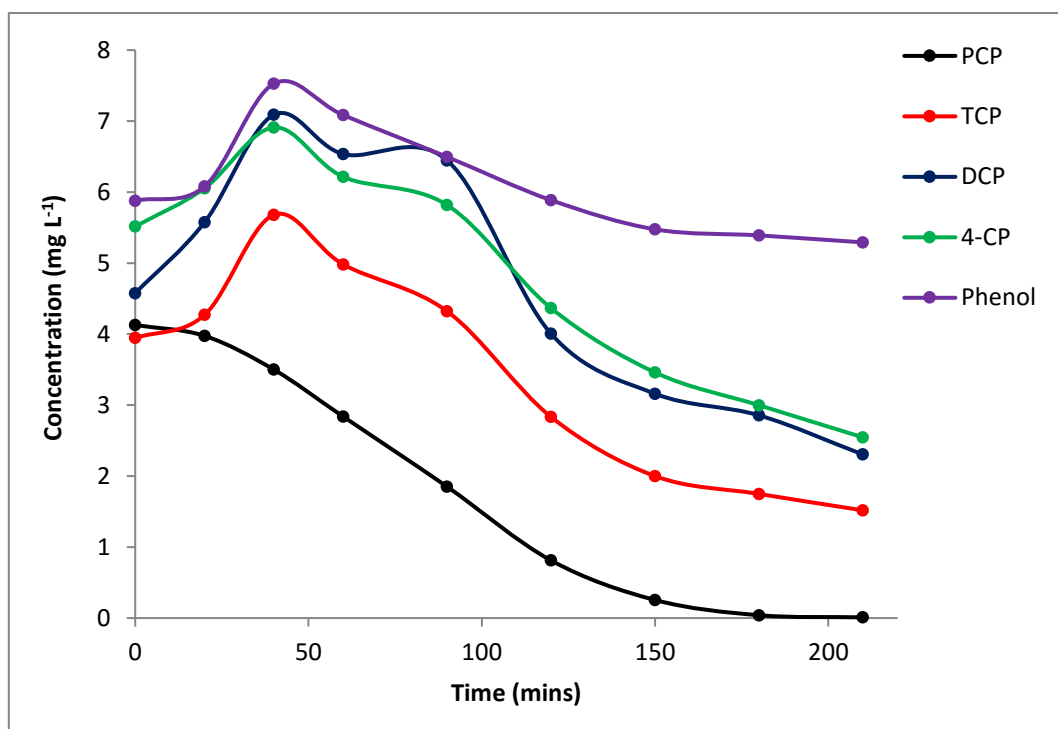
Figure 2.13: Photocatalytic degradation profiles of polychlorinated phenolics, C_o 5 mg L^{-1}

It is important to take into consideration the accumulative effect of lower-level substituted compounds at the expense of higher-level substituted compounds in the plotted profiles, this phenomenon will be analysed in more detail in sections to follow. It is clearly evident from Figure 2.16 that PCP has the best degradation efficiency, recording near 100 percent reduction in 180 minutes of irradiation.

TCP is the next in degradation efficiency, achieving over 60 percent reduction in 210 minutes of radiation exposure, while DCP and 4-CP managed reduction percentages of 50 and 54 respectively in the same period. Phenol expectedly was oxidised the poorest in comparison to the chlorinated phenolics, recording only 10 percent reduction. It should be noted that the calculated reduction percentage values of the analytes are done so strictly using the differences between initial instruments detected concentrations and the final recorded values, not taking into account the differential increases in concentrations of individual compounds from transformative contribution in the oxidation process, this dynamic will be the focus of sections to come.

It stands to reason that without an accumulative factored influence the recorded values might not read the same, but the dehalogenation sequence order should not be impacted to the point of drastic modification that may upset the order, especially for PCP, TCP, and Phenol. DCP and MCP profiles show a less definite order of oxidation, though this might be contributed to various possible errors at this point of the argument. To further interrogate the findings depicted in Figure 2.16 and to verify the hypothesised idea that higher-level substituted polychlorinated phenolics are better efficiently photocatalysed than lower-level substituted chloro-phenolics,

the PCP initial concentration was tripled to 15 mg L^{-1} while the other analyte initial concentration were kept at 5 mg L^{-1}.

Figure 2.17 shows the resulting oxidation profiles with the tripled PCP initial concentration. Even with the initial chemical concentration three-times that of the other analytes, PCP was reduced to near completeness in 200 minutes of irradiation. The TCP profile only manages near complete reduction in 270 minutes of light exposure. The phenol profile similarly to Figure 2.16 recorded the least removal, and interestingly, its percentage reduction was calculated to be 14 percent, which is not far off from the value recorded in the Figure 2.16 experimental set.

DCP and MCP profiles, though better pronounced in favour of the higher chlorinate compound, they do not represent conclusive substitution dependant oxidation. This inconclusiveness is validated by the deduced knowledge and expectation that 4-CP is a subsequent derivative of the oxidation degradation process of 2,4-DCP that would fractionally increase the presence of 4-CP in solution. Perhaps the chemical kinetic modelling determinations may provide clarity on the indifference in the dehalogenation sequence order between DCP and MCP.
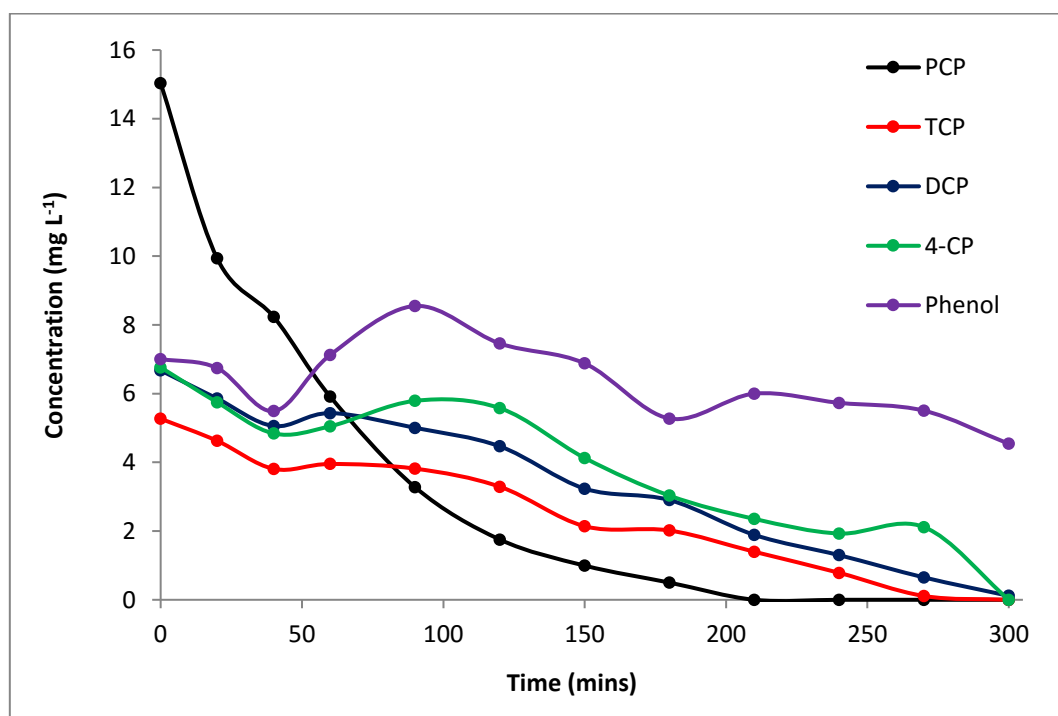

Figure 2.14: Photocatalytic degradation profiles of polychlorinated phenolics, [PCP]$_o$ 15 mg L^{-1}, all others C_o 5 mg L^{-1}

2.4.8 Dechlorination substitution mechanism

The proposed mechanism given by Augugliaro et al. (2012) for the photocatalytic degradation of aromatic compounds such as polychlorophenols is the substitution of chloro-halide species by hydroxyl groups. This oxidation mechanism was also validated by Taicheng et al. (2015) who found that $^{\circ}$OH was the major contributor to the photocatalytic degradation process of the analytes in that study. When the proposed mechanism is applied, a less halogenated chlorophenol compound is generated from the reaction of the higher-level substituted chlorophenol in the presence of oxygen molecules. Eq.6. shows the intermediate substitution step in oxidation dechlorination of pentachlorophenol to form tetrachlorophenol. The oxidation of the hydroxyl-group results in the introduction of tetrachlorophenol to the system. It is positively assumed that the multiple steps that follow in the oxidation process towards complete mineralisation follow suit.
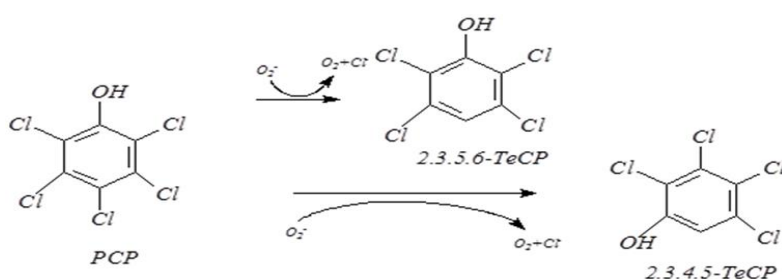
(Eq. 6)

2.4.9 Chemical transformation model

The acquired batch system simultaneous chemical profile outputs reflected specific behaviour across most determinations. This behaviour with the exception of PCP did not strictly conform to the Langmuir-Hinshelwood kinetics associated with adsorption driven facilitated oxidative degradation. With closer scrutiny it was apparent that there were distinctive time-course behavioural intricacies that were consistent with each particular analyte. Figure 2.18 shows profile fragments that were found to encompass multiple processes that outline the predominant transformation processes at different stages.
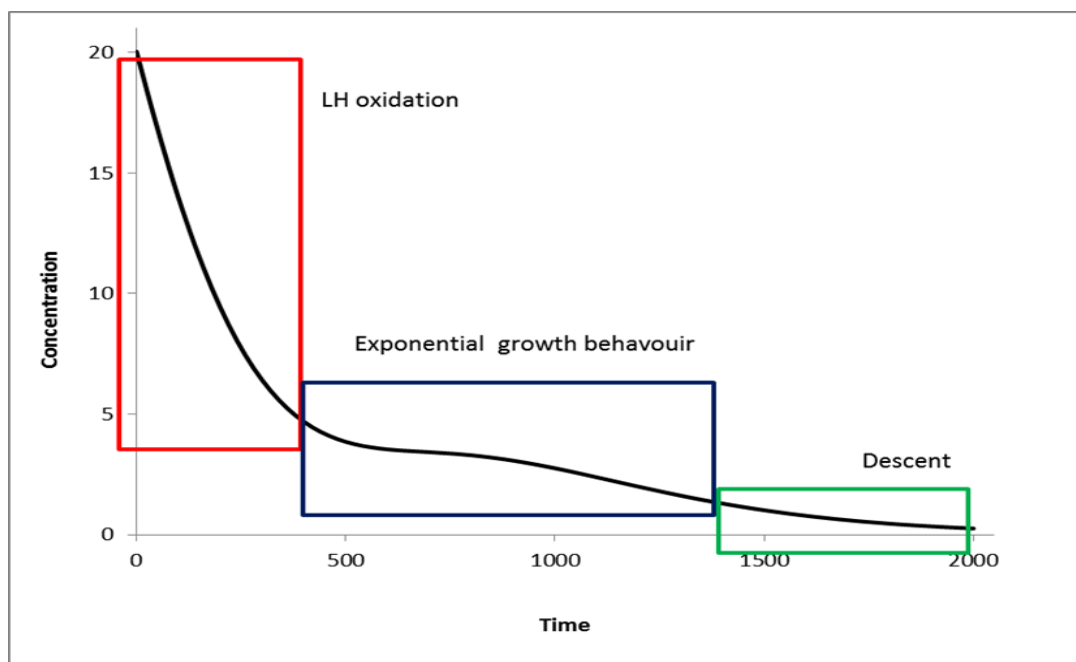
Figure 2.15: Time course profile transformations

The initial process boxed from time zero to time 400 minutes in Figure 2.18 is expected to be typified by the Langmuir-Hinshelwood model, red boxed. Figure 2.19 represents the simulated photocatalytic profiles that are calculated from the L-H expression, with continuation beyond 400 minutes whilst negating the influence of the exponential growth contributions that are shown separately in Figure 2.20. Figure 2.21 shows the combined simulated transformation profiles

The profile midsection boxed in Figure 2.18 shows the concentration accumulation exponential increases in the system that is represented separately in Figure 2.18, blue boxed. Eq. 7 is the exponential expression used to model the accumulative effects of intermediate derived compounds from the conversion of the higher chloride-substituted phenols. The last observed process of Figure 2.18 is the profile descent, green boxed. This behaviour is experienced when higher-level substituted analytes approach near complete depletion.

It is envisaged that once the oxidation process is completed for that particular adsorbed compound, provided that there are no derivative species with higher propensity of surface adsorption in solution, the sites are vacated and available for the next rank of compound in the systematic packing order. An increase in available sites improves mass transfer of lower level chloride analytes remaining in solution, which results in improved photocatalytic efficiencies.

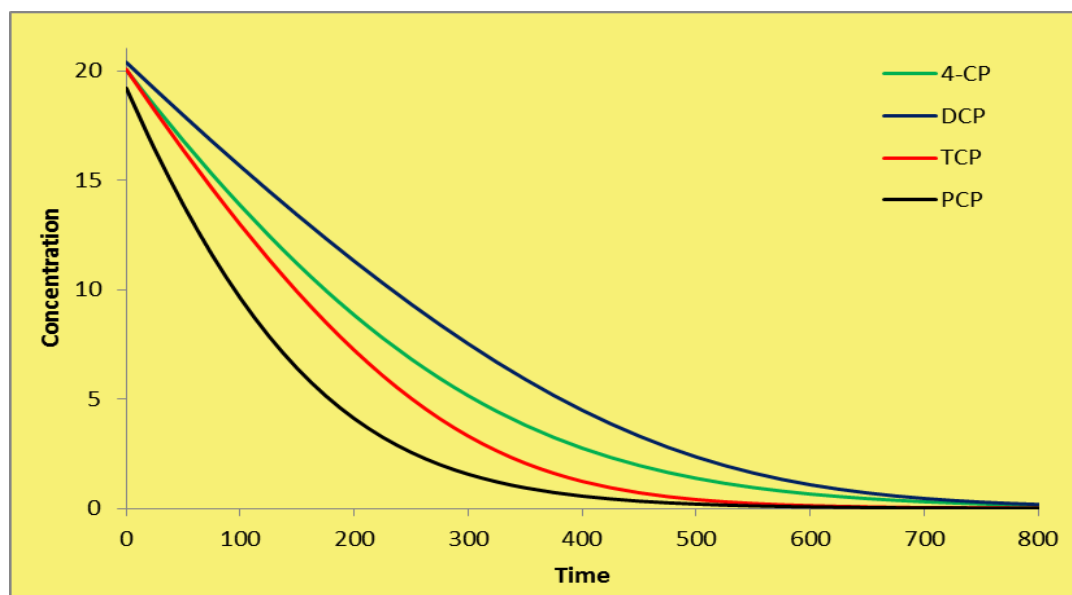$$C_n = \{C_{(n+1)_0} - C_{(n+1)_t}\} \; x \; exp^{k_{2n} \, x \, t} \hspace{5cm} \text{(Eq.7)}$$

Figure 2.16: Simulated photocatalytic oxidation when exponential growth contributions are negated
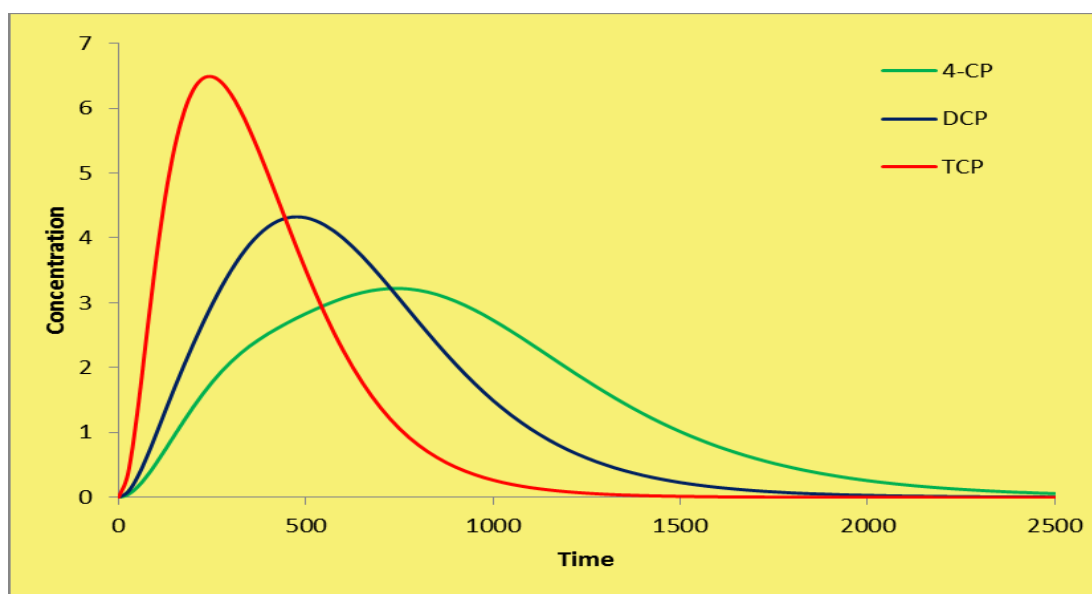

Figure 2.17: Simulated cumulative concentration contributions to the oxidation profiles
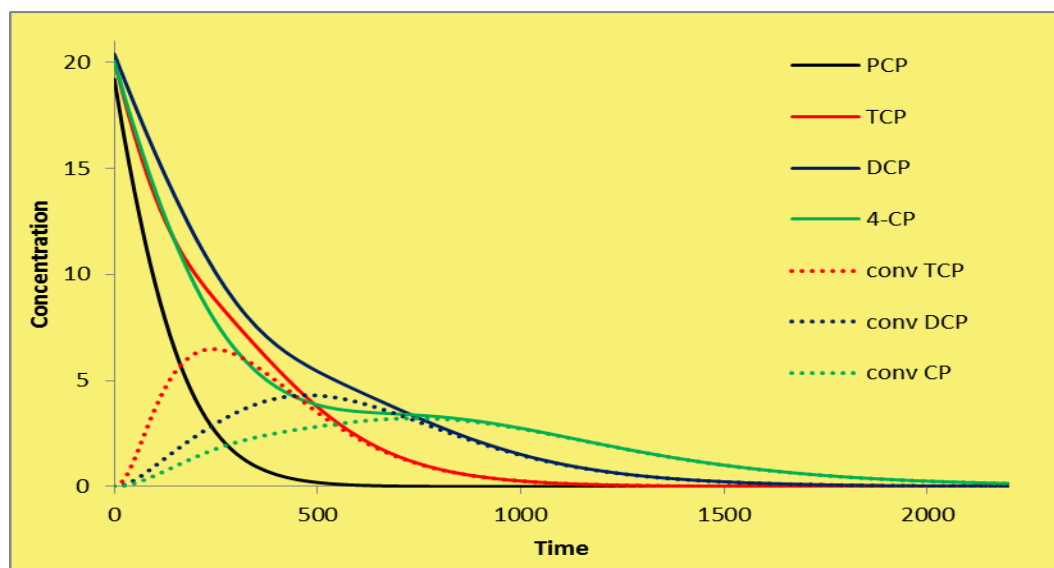
Figure 2.18: Combined simulated transformation profiles

Figure 2.22 shows the formation probability of the compounds of interest derived from the oxidation of high level substituted phenolics. The starting compound in the representation is PCP with subsequent formations of several TeCP isomers. This is followed by the statistical derivation of TCP's, DCP's and monochlorophenol isomers. From a statistical perspective, it is expected that the formation and accumulation of the resulting lower-level chlorophenols would not necessarily achieve population numbers in greater proportions to other isomers of the same substitutions.

Findings suggested that the populations of the analytes of interest were greater than those of their competing isomers, this is not a surprise given that the analytes of interest were selected based on their stability in aquatic systems at lower concentration ranges. This however does not suggest that the formation of competing isomers is altogether absent or that other mechanistic oxidation pathways are not undergone that may favour alternate routes, it is simply a matter of population numbers, where the most abundant species make up the bulk of variance.

In reality, many mechanistic pathways may be followed in the degradation processes that are dependent on many factors, which are speculated to be mostly influenced by project situational conditions. Under most advance oxidation conditions, multiple destructive processes are at play simultaneously and are governed by various dynamic processes. For example, it is likely to a small degree that photolysis with its many mechanism specific degradation pathways is responsible for a fraction of the transformations detected in analyte concentrations. This may entail photolytic specific dechlorination, dehydrogenation, aromatic ring splitting, and double bond saturation amongst other processes.

This may results in hosts of different intermediates that may include the analytes in question, the resulting detection does not differentiate the oxidation process responsible, but the efficiency of photocatalysis as the overriding process. In such cases, the photocatalytic mechanism is the far superior process and credit is placed primary on its performance. Photocatalysis oxidation may also follow multiple simultaneous degradation processes, some similar to photolysis, resulting in more products than those typified in this study. The underlining observation is that, the population measurements of the analytes under scrutiny far outweighs those of less stable isomers, and the time course profiles of the compounds oxidation agree with the model presented.
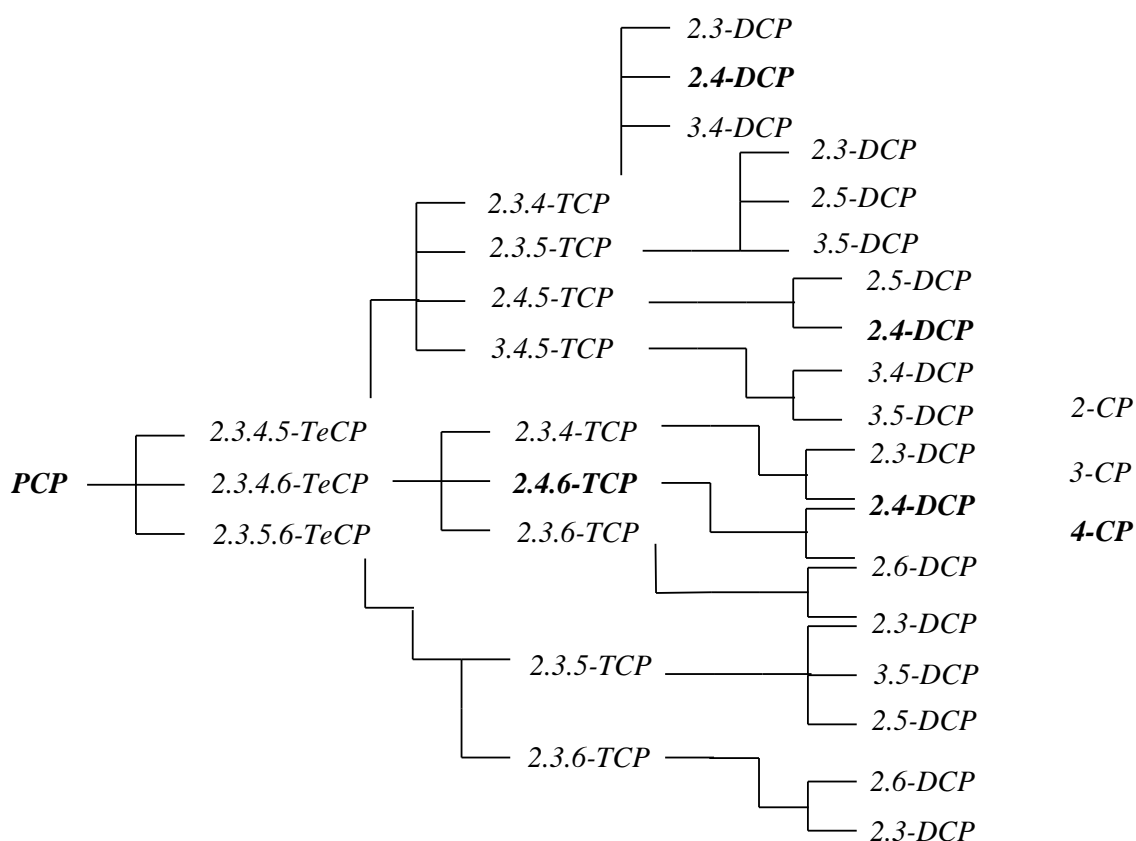
Figure 2.19: Derivative chemical probability tree of formation

2.4.10 **Transformation models fit**

The merge of Eq.7 and Langmuir-Hinshelwood expression takes the form of Eq.*8*, this equation describes kinetic time-course profiles that are representative of the recorded processed data for batch photocatalytic degradation experimental studies.

$$r \quad = \quad \frac{k_n \, K_n \, (C_n + \, (C_{(n+1)o} - C_{(n+1)t}) \,.\, Exp^{(kn2 \,.\, t)})}{1 + K_n \, (C_n + \, (C_{(n+1)o} - C_{(n+1)t}) \,.\, Exp^{(kn2 \,.\, t)})}$$

(Eq. 8)

The goodness of fit of the model and experimental data plots of each chloro-substituted analyte compound are shown in Figures 2.23-2.26. The batch system with the better fitting was selected to elucidate and validate the proposed model agreeability with data plots. Residual variations in the data presented do not significantly stray from those simulated using the model estimates.

Figure 2.20: PCP goodness of fit model versus recorded data

Figure 2.21: TCP goodness of fit model versus recorded data
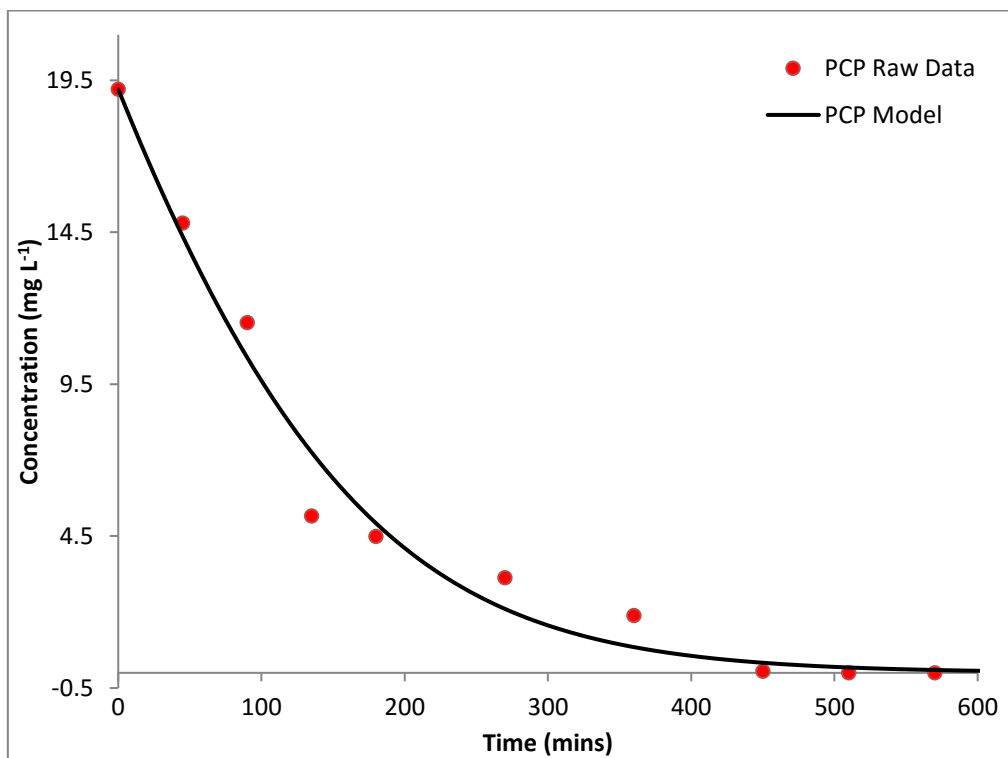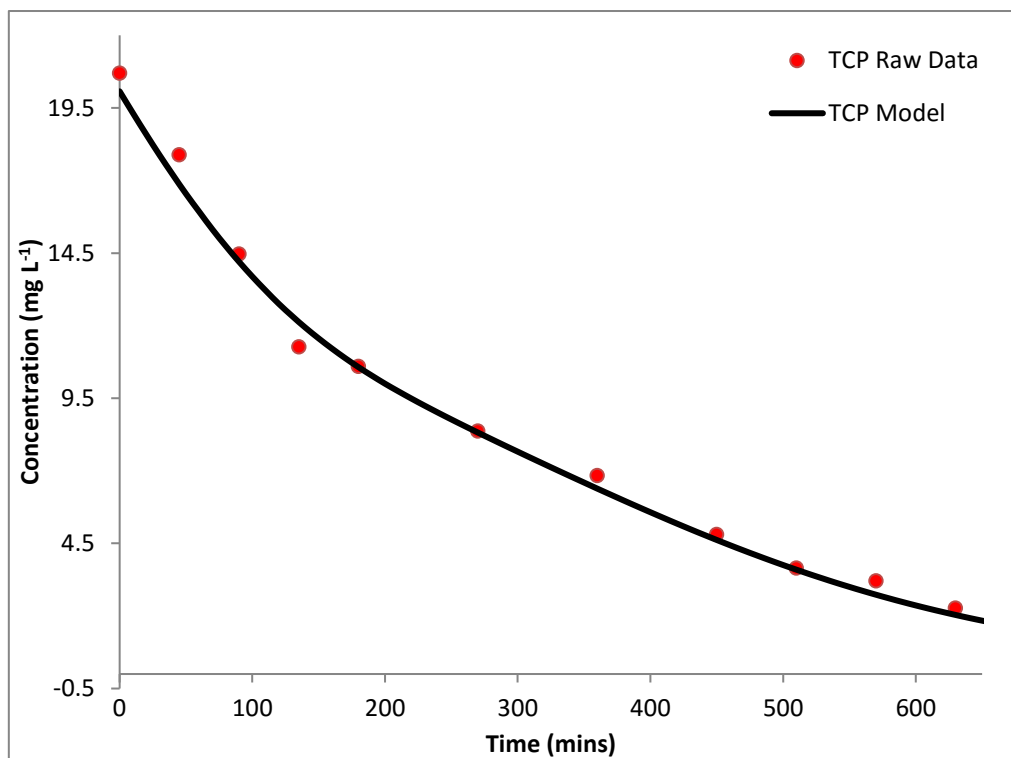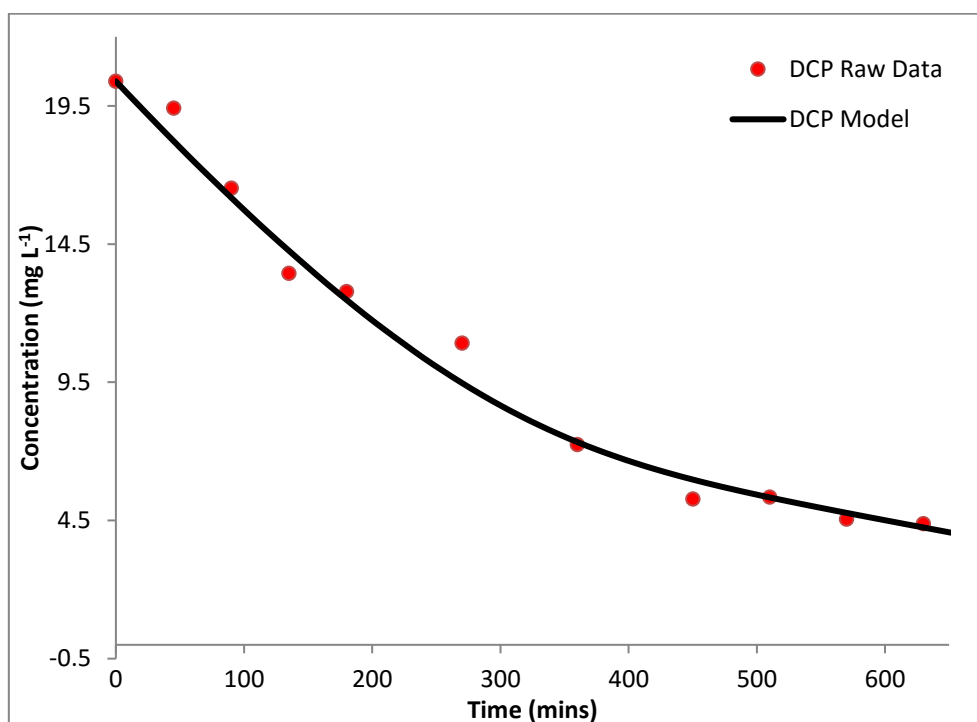

Figure 2.22: DCP goodness of fit model versus recorded data
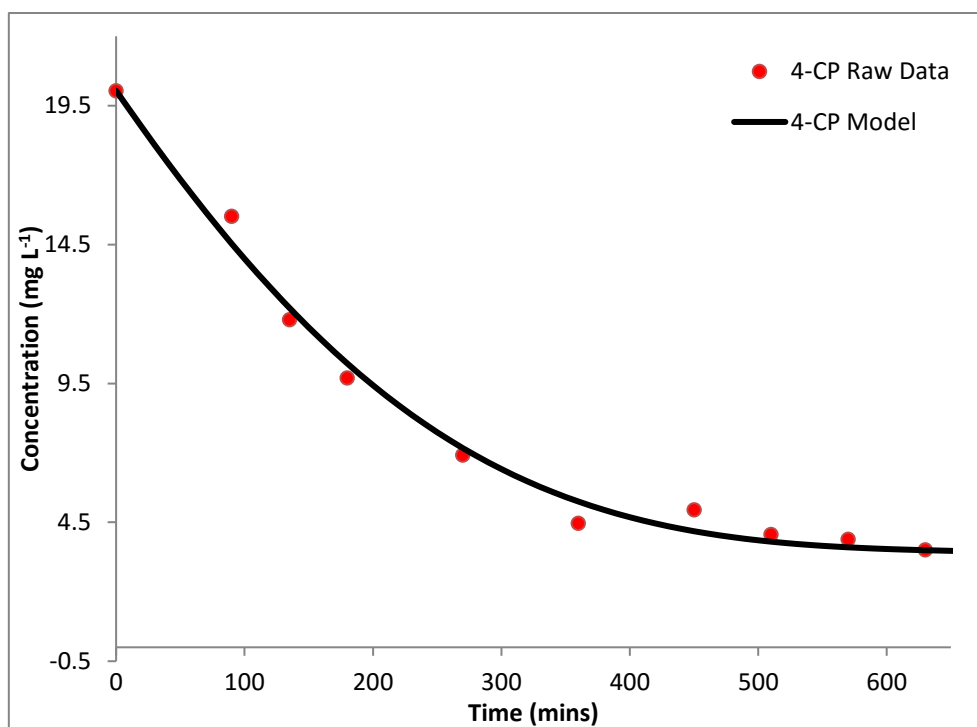
Figure 2.23: CP goodness of fit model versus recorded data

2.4.11 Batch system kinetic models

Figure 2.27 shows graphical plots of the simultaneous photocatalytic degradation of polychlorinated phenols in experimental batch systems. The estimated parameters of the models are recorded in Table 2.5 Pentachlorophenol's subsequent degradation results in the conversion and formation of a lower level chlorinated compound (TCP) amongst other derivative chemicals not included in the equation. The formation and concentration contributions from higher level chlorinated compounds to lower level chlorinated compounds are theoretically challenging to quantify. In this study, experimental data based models were used to estimate the contributions of higher level chlorinated phenolics to lower level compounds by applying chemical simulation techniques.

Table 2.5: Photocatalytic estimated parameters of phenolic compounds using the Langmuir-Hinshelwood

Parameter		MCP	DCP	TCP	PCP
K_L (mg L^{-1})		0.06756	0.14646	0.10892	0.03890
k(mg L^{-1}min^{-1})		0.11668	0.06560	0.11108	0.27392
k_2 (mg L^{-1}min^{-1})		0.00092	0.00150	0.00500	
C_o(mg L^{-1})		20.20432	20.3906	20.7000	19.2000

Figure 2.24: Simulated simultaneous photocatalytic degradation profiles of multi-chlorinated substituted phenolics

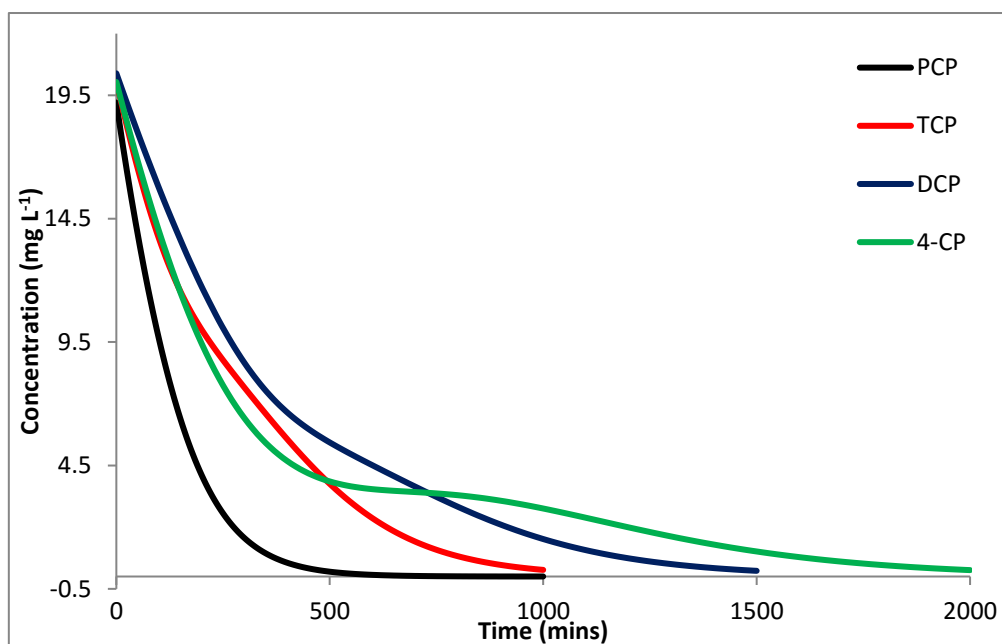Eq.*8* is the accumulation expression that is adapted into the Langmuir-Hinshelwood model as a function of concentration, and the rate of formation of lower derived chlorophenols at the expense of source compounds. Eq.*8* represents the total compound concentrations present in solution, which is the un-oxidised concentration remaining from the initial prepared solution and the addition of process derived chlorophenols taking into accounts principles of the exponential chemical growth to maximum model. When viewed closely, the data indicates three situations; (i) degradation of higher chlorinated compounds (PCP) alongside simultaneous degradation of lower level chlorinated compounds (TCP), (ii) the profile differentiation of lower level substituted chlorophenols from higher levels substituted chlorophenols due to formation and accumulation resulting from the converted higher substituted compounds, this is indicated by the bloated middle section of the profile, (iii) upon complete degradation and conversion of the higher level chlorophenol such as PCP, an improved removal efficiency of the lower level chlorinated compound such TCP is seen towards near complete removal point. This phenomenon is similar for the remaining chlorophenols in solution, the difference lies in the rate of degradation of each chlorophenol and the rate of introduction of the compound from the converted and depleted higher substituted compounds. 4-chlorophenol and 2.4-dichlophenol present an interesting dynamic, recorded experimental data suggests that MCP has a higher propensity for oxidation than DCP under the experimental conditions, though MCP is a derivative compound of the conversion process of DCP. Though MCP is constantly introduced into solution from the conversion of DCP, it is only in the latter periods of illumination where a distinct separation takes place. The influence of irradiation intensity is better depicted by the PCP degradation rate constants calculation, being the highest substituted phenolic analyte, PCP is only influenced by the Langmuir-Hinshelwood performance dynamics. The estimated Langmuir adsorptions constants do not deviate significantly from the calculated values.

CHAPTER 3: CONCLUSION AND RECOMMENDATIONS

3.1 CONCLUSIONS

The study focus was on experimental intricacies of heterogeneous semiconductor photocatalysis in the oxidation and treatment of polychlorinated substituted phenolic compounds as a representative class of chemicals. Titanium dioxide was the semiconductor photocatalyst of interest. The main study objective was to determine chemical transformation kinetics of multiple pollutant representative compounds that are simultaneously treated using photocatalytic advanced oxidation technology in aqueous systems. The motivation of the investigations was the optimisation of the photocatalytic treatment process. Without knowledge of the intricate behaviour and chemical interactions of many pollutant classes that constitute the typical wastewater and water discharges, efficiency in treatment and performance will not be realised.

The single compound oxidation efficiencies of the differently chloride substituted phenols showed that higher level substituted compounds were progressively less efficiently removed. The sequence of efficiency in compound disappearance was determined to be 4-CP > 2.4-DCP > 2.4.6-TCP > PCP > Phenol. Phenol is a route compound for the formation of chlorophenols, it was expectedly confirmed and in agreement to reported literature in that it is the least susceptible compound to oxidation in comparison to its substituted relation compounds.

The conclusions with regards to the findings in the study are that:

- The degradation of simultaneously oxidised chlorophenols and phenol recorded a reverse sequence to that of single compound determinations, with the exception of phenol, which remained the least efficient in oxidation. PCP being the highest substituted compound was degraded at a much faster rate than the less substituted phenolics, TCP followed suite, but at higher mass transfer conditions (suspended catalyst) there was no obvious significant difference in the efficiency of DCP and 4-CP degradation under the experimental conditions, though closer qualitative inspection of the data suggest that DCP was next in the oxidation sequence (PCP > TCP > DCP > 4-CP > Phenol). Under compromised photon efficiency and mass transfer conditions (glass immobilised catalyst) the sequence was true in favour of DCP. It can be concluded that the availability surface sites and photon delivery efficiency has a major influence on the oxidation of chlorophenols.

- The chemical transformations of simultaneously photocatalysed polychlorinated substituted phenols are fractionally accumulative at the expense of others, which means that the consumption of higher level substituted chlorophenols led to an increase in the concentrations of lower level substituted chlorophenols. The Langmuir-Hinshelwood expression required modification to incorporate population

growth dynamics that could explain this behaviour. The estimated Langmuir-Hinshelwood adsorption constant of the continuous flow system did not deviate too significantly from the ones calculated in batch processes.

3.2 RECOMMENDATIONS

The findings in this study provided insight on the complicated nature of heterogeneous photocatalytic reactions. The dehalogenation oxidation process that was tracked is just one of many probable reactions undergone on the surface of semiconductor photocatalyst resulting in decomposition of pollutants chemicals species found dissolved in natural waters.

Each class or group of compounds may not necessarily follow the same reaction scheme due to many factors that influence the photocatalytic mechanism. It would therefore be recommended that many determinations be performed on diverse groups of chemical compounds. This would provide information that could be used to classify and qualify the predominant routes followed towards complete mineralisation of organic pollutants.

It is also recommended that interrogation of matrices comprising of differing groups of unrelated and related compounds be conducted to establish statistical experimental probabilities with regards to parameters such as selectivity, reaction limits and hindrances. Disappearance of preselected compounds in treatment systems may not just indicate oxidation that follows strict reaction regimes, but rather many possibilities that may not be apparent in investigation designs and methodologies.

LIST OF REFERENCES

1. Ângelo, J., Andrade, L., Madeira, L.M. and Mendes, A. (2013). An overview of photocatalysis phenomena applied to NOx abatement, Journal of Environmental Management. 129. p522-539.

2. Augugliaro, V., Bellardita, M., Loddo, V., Palmisano, G., Palmisano, L. and Yurdakal, S. (2012). Overview on oxidation mechanisms of organic compounds by TiO_2 in heterogeneous photocatalysis, Journal of Photochemistry and Photobiology C: Photochemistry Reviews. 13. p224-245.

3. Bandara, J., Mielczarski, J.A., Lopez, A. and Kiwi, J. (2001). Sensitized degradation of chlorophenols on iron oxides induced by visible light: Comparison with titanium oxide, Applied Catalysis B: Environmental. 34. p321-333.

4. Batzill, M. (2001). Fundamental aspects of surface engineering of transition metal oxide photocatalysts, Energy and Environmental Science. 4. p3275-3286.

5. Benitez, F.J., Beltrán-Heredia, J., Acero, J.L., Rubio, F.J. (2000). Rate constants for the reactions of ozone with chlorophenols in aqueous solutions, Journal of Hazardous Materials. 79. p271-285.

6. Carp, O., Huisman, C.L. and Reller, A. (2004). Photoinduced reactivity of titanium dioxide, Progress in Solid State Chemistry. 32. p33-177.

7. Chen, D., Sivakumar, C., Ray, A.K. (2000).Heterogeneous photocatalysis in environmental remediation, Dev. Chemical Engineering Mineral. Processes. 8. p505-550.

8. De Lasa, H., Serrano, B., Salaisis, M. (2005). Photocatalytic reaction engineering, Springer Science, New York.

9. Demeestere, K., Dewulf, J. and Van Langenhove, H. (2007). Heterogeneous Photocatalysis as an Advanced Oxidation Process for the Abatement of Chlorinated, Monocyclic Aromatic and Sulfurous Volatile Organic Compounds in Air: State of the Art, Critical Reviews in Environmental Science and Technology. 37. p489-538.

10. Esparza, P., Borges, M.E., Díaz, L., Alvarez-Galván, M.C., Fierro, J.L.G. (2010). Photodegradation of dye pollutants using new nanostructured titania supported on volcanic ashes, Applied Catalysis A: General. 388. p7-14.

11. Giles, C.H., MacEwan, T.H., Nakhwa, S.N. and Smith, D. (1960). Studies in adsorption. Part XI. A system of classification of solution adsorption isotherms, and its use in diagnosis of adsorption mechanisms and in measurements of specific surface areas of solids, Journal of Chemical Society. 10. p3973-3993.

12. Hamdaoui, E., Naffrechoux. (2007). Modeling of adsorption isotherms of phenol and chlorophenols onto granular activated carbon: Part I. Two-parameter models and equations allowing determination of thermodynamic parameters, Journal of Hazardous Materials. 147. p381-394.

13. Inagaki, M., Kang, F., Toyoda, F. and Konno, H. (2014). Chapter 13: Carbon Materials in Photocatalysis, M.I.K.T. Konno (Ed.), Advanced Materials Science and Engineering of Carbon, Butterworth-Heinemann, Boston. p289-311.

14. Jin, L. and Dai, B. (2012). TiO2 activation using acid-treated vermiculite as a support: Characteristics and photoreactivity, Applied Surface Science. 258. p3386-3392.

15. Lathasree, S., Rao, A.N., SivaSankar, B., Sadasivam, V., Rengaraj, K. (2004). Heterogeneous photocatalytic mineralisation of phenols in aqueous solutions, Journal of Molecular Catalysis A: Chemical. 223. p101-105.

16. Lazar, M.A., Varghese, S., Nair, S.S. (2012). Photocatalytic water treatment by titanium dioxide: recent updates, Catalysts. 2. p572-601.

17. Michałowicz, J. and Duda, W. (2007). Phenols-sources and toxicity, Polish Journal of Environmental Studies, 16 (3). p347-362.

18. Mohseni, M. and Taghipour, F. (2004). Experimental and CFD analysis of photocatalytic gas phase vinyl chloride (VC) oxidation, Chemical Engineering Science. 59. p1601-1609.

19. Nugraha, J. and Fatimah, I. 2013). Evaluation of photodegradation efficiency on semiconductor immobilized clay photocatalyst by using probit model approximation, International Journal of Chemical and Analytical Science. 4. p125-130.

20. Oller, S.M. and Sanchez-Perez J.A. (2011). Combination of advanced oxidation processes and biological treatment for wastewater decontamination: A review, Science of The Total Environment. 409. p4141-4166.

21. Pelentridou, K., Stathatos, E. and Karasali, Lianos, P. (2009). Photodegradation of the herbicide azimsulfuron using nanocrystalline titania films as photocatalyst and low intensity Black Light radiation or simulated solar radiation as excitation source, Journal of Hazardous Materials. 163. p756-760.

22. Pera-Titus, M., García-Molina, V., Banos, M.A., Giménez, J., Esplugas, S. (2004). Degradation of chlorophenols by means of advanced oxidation processes: A general review, Applied Catalysis B: Environmental. 47. p219-256.

23. Pozzo, R.L., Baltanás, M.A., Cassano, A.E. (1997). Supported titanium oxide as photocatalyst in water decontamination: State of the art, Catalysis Today. 39. p219-231.

24. Reichert, P. (Ed.). (1998).Aquasim 2.0-User Manual, Swiss Federal Institute for Environmental Science and technology, CH 8600, Dubendorf, Switzerland.

25. Song-hu, Y. and Xiao-hua, L. (2005). Comparison treatment of various chlorophenols by electro-Fenton method: relationship between chlorine content and degradation, Journal of Hazardous Materials. 118. p85-92.

26. Taicheng, A., Jibin, A., Yanpeng, G., Guiying, L., Hansun, F. and Weihua, S. (2015). Photocatalytic degradation and mineralization mechanism and toxicity assessment of antivirus drug acyclovir: Experimental and theoretical studies, Applied Catalysis B: Environmental. 164. p279-287.

27. World Health Organisation. (2008). A Snapshot of Drinking Water and Sanitation in Africa, WHO/UNICEF Joint Monitoring Programme for Water Supply and Sanitation.

28. Yasmina, M., Mourad, K., Mohammed, S.H., Khaoula, C. (2014). Treatment Heterogeneous Photocatalysis; Factors Influencing the Photocatalytic Degradation by TiO2, Energy Procedia. 50. 559-566.

29. Zhonghua, H. and Vansant, E.F. (1993). Adsorption of phenol and chlorophenols from aqueous solution by modified elutrilithes, Catalysis Today. 17. p41-51.